Ecotoxicology and Environmental Safety 319 (2026) 120310

Contents lists available at ScienceDirect

Ecotoxicology and Environmental Safety

journal homepage: www.elsevier.com/locate/ecoenv

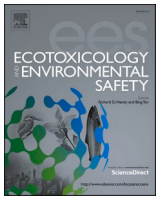

From tooth to gut: Proteomic evidence of systemic dysregulation in fluorosis

Nawapan Pongsapipatana [a], Patcharaporn Gavila [a,b], Thutchima Khieota [a], Han-Sung Jung [c], Hamid Alinejad-Rokny [d,e], Sung-Dae Cho [f], Kanokwan Sriwattanapong [a,g,*], Thantrira Porntaveetus [a,h]

[a] Center of Excellence in Precision Medicine and Digital Health, Department of Physiology, Faculty of Dentistry, Chulalongkorn University, Bangkok 10330, Thailand
[b] Intercountry Centre for Oral Health, Department of Health, Ministry of Public Health, Chiangmai 50000, Thailand
[c] Division in Anatomy and Developmental Biology, Department of Oral Biology, Taste Research Center, Oral Science Research Center, Yonsei University College of Dentistry, Seoul, Korea
[d] UNSW BioMedical Machine Learning Lab (BML), School of Biomedical Engineering, UNSW Sydney, Sydney, NSW 2052, Australia
[e] Visiting Scholar (Collaborative Projects), Center of Excellence in Precision Medicine and Digital Health, Chulalongkorn University, Bangkok 10330, Thailand
[f] Department of Oral Pathology, School of Dentistry and Dental Research Institute, Seoul National University, Seoul 03080, Republic of Korea
[g] Oral Biology Research Center, Faculty of Dentistry, Chulalongkorn University, Bangkok 10330, Thailand
[h] FutureDent Digital Center, Faculty of Dentistry, Chulalongkorn University, Bangkok 10330, Thailand

ARTICLE INFO

Keywords:
Fluorosis
Healthcare access
Toxicity
Proteomics
Environmental exposure

ABSTRACT

Excessive fluoride intake during early tooth development causes dental fluorosis, yet chronic high fluoride exposure may also disrupt gastrointestinal physiology and host–microbe interactions. We profiled the host fecal proteome of school-aged children with severe dental fluorosis (PF; TF 5–9; n = 10) and age-matched controls (CF; TF 0; n = 10) from a fluoride-endemic region of Thailand, with systemic exposure confirmed by elevated 24-h urinary fluoride excretion. LC–MS/MS identified 182 proteins (164 retained after filtering), including 24 proteins detected exclusively in PF samples. Differential protein expression revealed six upregulated (C3, FYTTD1, TRIP11, PRDX4, CDH1, SI) and four downregulated (SIAE, ZG16, MUC5AC, GUSB). Enrichment analyses implicated coordinated alterations in epithelial adhesion and barrier regulation, vesicular trafficking/ER proteostasis, oxidative stress responses, carbohydrate metabolism, and innate immune signaling. Knowledge-based interaction mapping (STRING/IntAct) further nominated cystic fibrosis transmembrane conductance regulator (CFTR)–centered epithelial ion-transport and barrier pathways as a convergent axis linking multiple fluoride-responsive proteins. These findings provide human proteomic evidence that fluorosis associates with intestinal epithelial and immune dysregulation extending beyond enamel pathology, supporting a systems-level view of fluorosis as a multisystem condition.

1. Introduction

Dental fluorosis is a developmental enamel defect characterized by hypomineralization resulting from excessive fluoride exposure during tooth formation (Rosas López Portillo et al., 2024). Although fluoride at optimal levels is indispensable for skeletal homeostasis and the prevention of dental caries, it is widespread in natural and anthropogenic sources, including drinking water, dietary components, and dental products (Gupta et al., 2025; Samaranayake et al., 2025). The recommended daily fluoride intake for effective caries prevention is approximately 0.05–0.07 mg F/kg body weight/day (Spencer et al., 2018). However, sustained fluoride exposure beyond this threshold perturbs ameloblast activity and interferes with enamel matrix deposition and maturation, ultimately resulting in fluorosis (Bronckers et al., 2009). Clinically, dental fluorosis exhibits a broad spectrum of severity, ranging from mild white opacities to moderate brown discoloration and, in severe cases, extensive surface pitting, enamel breakdown, and dark brown to black staining. In addition to its aesthetic impact and potential psychosocial burden, advanced fluorosis can significantly impair enamel strength and compromise normal dental

* Corresponding author at: Center of Excellence in Precision Medicine and Digital Health, Department of Physiology, Faculty of Dentistry, Chulalongkorn University, Bangkok 10330, Thailand.
E-mail address: kanokwan.sr@chula.ac.th (K. Sriwattanapong).

https://doi.org/10.1016/j.ecoenv.2026.120310
Received 9 February 2026; Received in revised form 8 May 2026; Accepted 21 May 2026
Available online 27 May 2026

function (Porntaveetus et al., 2017; Rosas López Portillo et al., 2024).

Over recent decades, the prevalence of fluorosis has increased worldwide, particularly in regions with naturally high fluoride levels in drinking water and inadequate monitoring of fluoride intake, including several areas in Southeast Asia and Thailand (Chuah et al., 2016; McGrady, Ellwood, Srisilapanan, Korwanich, Taylor, et al., 2012; McGrady, Ellwood, Srisilapanan, Korwanich, Worthington, et al., 2012; Nakornchai et al., 2016; Rojanaworarit et al., 2021). This growing public health burden highlights the urgent need to understand not only the dental consequences of fluoride exposure but also its broader biological and systemic effects. Following ingestion, fluoride is rapidly absorbed through the gastrointestinal tract, with approximately 75–90% entering systemic circulation. Nearly 99% of absorbed fluoride is deposited in calcium-rich tissues such as bones and teeth, while a fraction accumulates in soft tissues including the gastrointestinal tract, kidneys, and spleen (Johnston and Strobel, 2020; Naghavi et al., 2025). Fluoride retention is markedly higher in children (80–90%) than in adults (~60%), increasing susceptibility to chronic toxicity during early life (Dec et al., 2017). Importantly, excessive fluoride exposure disrupts intestinal epithelial integrity, induces oxidative stress, and activates inflammatory signaling pathways, including NF-κB and JAK/STAT, resulting in impaired mucosal barrier function and altered intestinal homeostasis (Amadeu de Oliveira et al., 2018; Liu et al., 2025).

Proteomic studies in animal models have demonstrated that fluoride induces region-specific molecular alterations along the intestinal tract, affecting cytoskeletal organization, vesicular trafficking, mitochondrial metabolism, neuronal signaling, and protein turnover (Dionizio et al., 2021, 2018; Melo et al., 2017). However, despite research on skeletal and dental effects of fluoride and growing mechanistic insight from animal intestines, proteomic investigations of chronically exposed human gastrointestinal samples remain extremely limited. A recent salivary proteomic study in patients with dental fluorosis reported dysregulation of cystic fibrosis transmembrane conductance regulator (CFTR)-associated proteins and reduced immune-related proteins, suggesting impaired ion transport and mucosal immunity in severe disease (Gavila et al., 2024). Beyond salivary changes, emerging human urinary proteomic evidence suggests that fluoride exposure is associated with alterations in proteins involved in biomineralization, extracellular matrix regulation, oxidative stress, and immune-inflammatory pathways, indicating broader systemic molecular disturbances in exposed children (Pongsapipatana et al., 2026). Nevertheless, whether similar molecular disturbances occur within the intestinal environment of fluorosis patients remains unknown.

Beyond its direct effects on host intestinal cells, fluoride exposure has been implicated in perturbations of gut microbial composition and metabolic activity (Yasin et al., 2025). Disruption of host–microbiota crosstalk, together with fluoride-induced proteomic remodeling of intestinal tissues, may amplify systemic inflammation, immune dysregulation, and metabolic imbalance, thereby contributing to extraintestinal manifestations of fluoride toxicity throughout the body. To address this critical gap, we performed host fecal proteomic profiling in school-aged children with severe dental fluorosis and age-matched controls living in a fluoride-endemic region. We quantified differential protein abundance and fluorosis-specific proteins, followed by functional enrichment and protein–protein interaction network analyses to identify pathways perturbed by chronic fluoride exposure and to nominate convergent signaling axes linking epithelial barrier function, mucosal immunity, and metabolism.

2. Material and methods

2.1. Subject recruitment and study design

Participants aged 6–14 years were recruited from fluoride-endemic areas in Ratchaburi province, Thailand, with the support of local schools and community health centers. Information sessions were conducted to explain the study's objectives, procedures, and potential benefits to both parents and children. Written informed consent was obtained from parents or legal guardians, and assent was obtained from all participating children prior to enrollment. Following recruitment, oral examinations were performed to assess dental fluorosis, and participants were classified into two groups: the control group (CF) and the fluorosis patient group (PF). Severe dental fluorosis was defined according to the Thylstrup and Fejerskov (TF) index, with CF participants assigned a TF score of 0 and PF participants assigned TF scores ranging from 5 to 9, in accordance with established criteria (Gavila et al., 2024; Silva de Castilho et al., 2009). Participant eligibility was determined using exclusion criteria previously reported by Gavila et al. (2024). Individuals were not included if they were presented with dental caries, systemic disorders, or amelogenesis imperfecta, or if they had used antibiotics, antifungal, antiviral, or steroid medications, as well as mouthwash, within 3 months prior to sample collection. Additional exclusion criteria included clinical signs of periodontitis or oral mucosal lesions, smoking, alcohol consumption, or a history of narcotic drug use.

2.2. Ethical approval

The study received approval from the Human Research Ethics Committee of the Faculty of Dentistry, Chulalongkorn University, Thailand (HREC-DCU 2021–064, approved on October 1, 2021) and adhered to the 1964 Helsinki Declaration and its subsequent amendments.

2.3. Fecal and urine samples collection

Fecal and urine samples were collected from participants in both the CF ($n = 10$) and the PF ($n = 10$) during scheduled school visits to ensure standardized and consistent sampling conditions. Fecal samples were collected in the morning using sterile, designated collection containers. To minimize contamination, participants were instructed to place clean sheet of toilet paper on the dry surface of the toilet bowl, defecate onto the paper, and then use the provided collection tools to transfer the upper portion of the feces into the container. All fecal samples were immediately stored on dry ice during transportation to preserve sample integrity. Samples were subsequently aliquoted into small tubes to prevent repeated freeze–thaw cycles and kept at −80 °C until analysis.

Urinary fluoride concentrations were assessed using 24-hour urine samples collected and measured (Gavila et al., 2024). The first morning void was discarded, and all subsequent urine output was pooled, transferred into screw-capped bottles, and stored on dry ice during transport. Fluoride concentrations were measured using a fluoride ion-selective electrode (4-Star Benchtop, Orion, USA) with total ionic strength adjustment buffer containing cyclohexylenedinitrilotetra acetate, sodium hydroxide, sodium chloride, and acetic acid. Urine samples were subsequently aliquoted into 1 mL volumes in 1.5-mL microcentrifuge tubes to prevent repeated freeze–thaw cycles and stored at −80 °C until analysis.

2.4. Liquid chromatography with tandem mass spectrometry (LC–MS/MS)

Fecal samples were lysed in lysis buffer containing 8 M urea in 100 mM triethylammonium bicarbonate (TEAB) supplemented with Halt protease inhibitor cocktail (Thermo Fisher Scientific, CA, USA), followed by incubation on ice for 2 h. The lysates were clarified by centrifugation at 14,000 × g for 20 min at 4 °C, and protein concentrations were determined using the Pierce™ BCA Protein Assay Kit (Thermo Fisher Scientific, CA, USA).

Proteomic profiling by LC–MS/MS was carried out at the Center of Excellence in Systems Biology, Faculty of Medicine, Chulalongkorn University, following a previously validated protocol (Makjaroen et al., 2018; Prawatvatchara et al., 2025; Techawiwattanaboon et al., 2023)

with some modifications. Protein samples (100 μL, approximately 100 μg) were reduced with 10 μL of dithiothreitol (DTT) at 37 °C for 30 min and subsequently alkylated with 40 μL of 100 mM iodoacetamide (IAA) in the dark at room temperature for 30 min. Excess IAA was quenched by adding 40 μL of 100 mM DTT and incubating at room temperature for at least 15 min. The urea concentration was then reduced from 8 M to < 1 M by dilution with 100 mM TEAB. Proteins were digested with trypsin at a 1:50 (w/w) enzyme-to-protein ratio at 37 °C for 16 h. The digestion was terminated by the addition of trifluoroacetic acid (TFA) to a final concentration of 0.5%, followed by incubation at room temperature for 15 min. Digested peptides were dried using a SpeedVac concentrator. Tryptic peptide concentrations were measured using the Pierce Quantitative Fluorometric Peptide Assay (Thermo Fisher Scientific, CA, USA). Peptides were subsequently labeled with TMT10plex™ isobaric reagents (Thermo Fisher Scientific, CA, USA) and fractionated using a high-pH reversed-phase peptide fractionation kit (Pierce). The resulting peptide fractions were dried and stored at −80 °C prior to analysis.

Before analysis, peptides were reconstituted in 0.1% formic acid (FA) and analyzed using an EASY-nLC 1000 system coupled to a Q-Exactive Orbitrap Plus mass spectrometer (Thermo Fisher Scientific, CA, USA) equipped with a 25-cm EASY-Spray C18 column (75 μm inner diameter). Peptide separation was performed using a 90-min gradient at a flow rate of 300 nL/min under the following conditions: 0–5% solvent B at 0 min, 5–20% B over 60 min, 20–40% B over 23 min, 40–95% B in 2 min, and held at 95% B for 5 min. An electrospray voltage of 2.0 kV was applied. Full MS1 spectra (m/z 350–1400) were acquired in the Orbitrap at a resolution of 70,000 with an automatic gain control (AGC) target of 3×10^6 and a maximum injection time of 250 ms. The top 10 most intense precursor ions were selected for fragmentation using a normalized collision energy (NCE) of 32. MS2 spectra were acquired at a resolution of 35,000 with an AGC target of 1×10^5 and a maximum injection time of 100 ms.

2.5. Data analysis and visualization

Raw mass spectrometry data were searched against the human Swiss-Prot database supplemented with a curated list of common protein contaminants. Peptide and protein identification, quantification, and normalization were performed using Proteome Discoverer™ software version 2.1 (Thermo Fisher Scientific, city, USA). To specifically isolate the host-derived proteome, MS/MS spectra were searched against the UniProt human reference proteome database (Taxonomy ID: 9606), excluding microbial sequences to ensure that the identified protein library reflects human biological responses at the mucosal–luminal interface in this study. The precursor and fragment ion mass tolerances were set at 10 ppm and 0.02 Da, respectively. Peptide-spectrum matches were filtered using a false discovery rate (FDR) of 1% at the peptide level during the protein identification (Techawiwattanaboon et al., 2023). This strategy minimizes false positives at the identification stage, ensuring that the reported protein library is highly reliable. Reporter ion intensity ratios for the CF and PF groups were $\log_2$-transformed prior to statistical analysis. Differential protein expression was assessed using independent t-tests, requiring a minimum of three valid $\log_2$ intensity values per group. Proteins with a p-value < 0.05 and an absolute $\log_2$ fold change ($|\log_2 FC|$) ≥ 0.5 were considered significantly differentially expressed. This criterion is widely accepted in discovery-phase studies to capture biologically meaningful alterations in complex clinical samples (Kim et al., 2021; Skates et al., 2013; Ting et al., 2009).

Functional analysis of the identified proteins was performed using Database for Annotation, Visualization and Integrated Discovery (DAVID) Bioinformatics Resources (https://davidbioinformatics.nih.gov/summary.jsp) (Sherman et al., 2022) to evaluate Gene Ontology (GO) enrichment, including biological processes (BP), molecular functions (MF), and cellular components (CC). Pathway enrichment analysis was conducted using databases including KEGG (https://www.kegg.jp/kegg/pathway.html) (Kanehisa et al., 2023), Reactome (https://reactome.org/) (Milacic et al., 2023), and WikiPathways (https://www.wikipathways.org/) (Agrawal et al., 2023). Protein–protein interaction (PPI) and network anaylsis were constructed using STRING (https://string-db.org/) (Szklarczyk et al., 2023) and the IntAct database (Orchard et al., 2013; Panneerselvam et al., 2024) through Cytoscape (Shannon et al., 2003). To ensure high-confidence interactions, the 'Combined Score' was used as the primary evaluation parameter for the STRING database, integrating evidence from experimental data, curated databases, and co-expression. A minimum interaction score of 0.400 (medium confidence) was applied to filter out low-probability associations. For the IntAct database, interaction confidence was assessed using the MIscore (SMI), a normalized score ranging from 0 to 1 that reflects the reliability of combined experimental evidence (Villaveces et al., 2015). Data visualization was performed using SRplot.

2.6. Statistical analysis

Statistical analyses were conducted using SPSS software version 22 (SPSS Inc., Chicago, IL, USA) and Microsoft Excel. The Mann–Whitney U-test was applied to compare age distributions between groups, while Fisher's Exact Test was used to assess differences in sex distribution. Independent t-tests were used for differential expression analysis in the proteomic dataset. Statistical significance was defined as $p < 0.05$.

3. Results

3.1. Participant characteristics and verification of fluoride exposure

Baseline demographic characteristics and urinary fluoride levels were evaluated to ensure group comparability and to validate systemic fluoride exposure prior to downstream proteomic analysis. An overview of the experimental and analytical workflow is illustrated in Fig. 1. The CF group consisted of 4 males and 6 females (n = 10), while the PF group comprised 3 males and 7 females (n = 10). There were no significant differences in age or sex distribution between the two groups, indicating appropriate demographic matching (Supplementary Table S1). Systemic fluoride exposure was subsequently verified by assessing 24-hour daily urinary fluoride excretion (DUFE) (Figs. 1B, 1C and Supplementary Table S1 and S2). Children in the PF group exhibited significantly elevated 24-h DUFE compared with the CF group, confirming substantially higher systemic fluoride exposure among PF group.

3.2. Alterations in the fecal proteomic profiles in fluorosis patients

A total of 182 proteins were identified from the fecal proteomic profiles of the CF and PF groups (Supplementary Table S3). Following the removal of contaminants and filtering for missing values, 164 proteins were retained for downstream analysis (Fig. 2A). Comparative analysis using a Venn diagram revealed that 24 proteins were uniquely detected in the PF group, whereas 140 proteins were commonly identified in both groups (Fig. 2B). Differential protein expression analysis highlighted 13 significantly altered proteins between the two groups (p-value < 0.05) (Fig. 2C, Table 1). Hierarchical clustering further demonstrated a clear segregation of CF and PF samples based on their proteomic profiles, revealing distinct expression patterns associated with fluorosis status (Fig. 2D). Differentially expressed proteins were defined using a $\log_2 FC$ threshold of either > 0.50 or < -0.50. Specifically, 6 proteins, Complement C3 (C3), UAP56-interacting factor (FYTTD1), Thyroid receptor-interacting protein 11 (TRIP11), Peroxiredoxin-4 (PRDX4), Cadherin-1 (CDH1), and Sucrase-isomaltase (SI), were significantly upregulated in the PF group (Fig. 3A–3 F). Conversely, 4 proteins, Sialate O-acetylesterase (SIAE), Zymogen granule membrane protein 16 (ZG16), Mucin-5AC (MUC5AC), and β-glucuronidase (GUSB), were significantly downregulated in PF group (Fig. 3G–3 J).

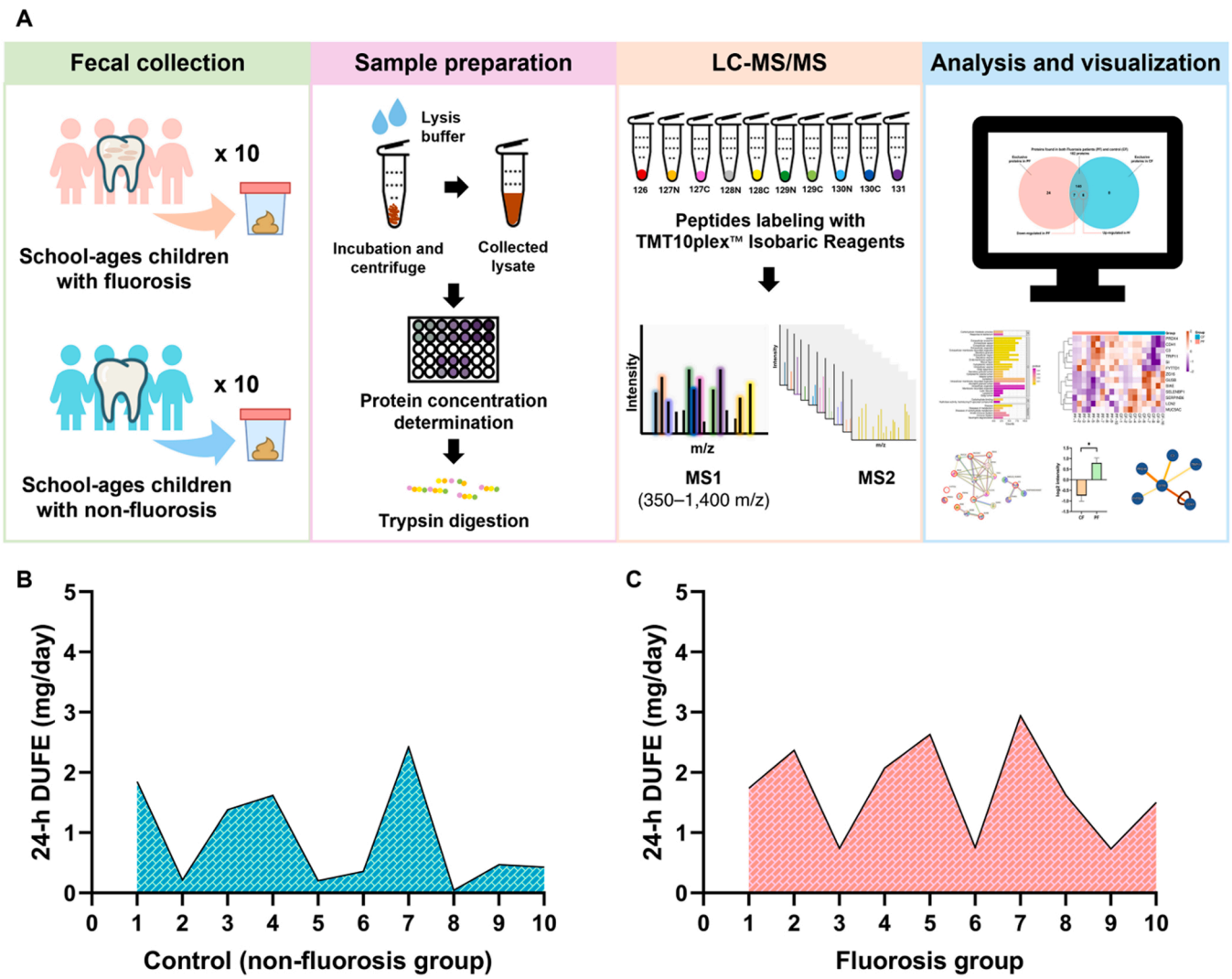

Fig. 1. Overview of the study design and fluoride exposure assessment. (A) Schematic illustration of the overall study workflow. (B) Comparison of 24-h DUFE between the CF and PF groups.

3.3. Functional enrichment and pathway analysis of differential fecal proteomic signatures in fluorosis patients

To elucidate the biological significance of fluoride-associated proteomic alterations, GO terms and pathway enrichment analyses were performed on the 10 significantly dysregulated proteins (Fig. 4A; Supplementary Table S4). BP of GO analysis revealed significant enrichment in pathways related to carbohydrate metabolic processes and host response to bacteria. CC of GO analysis demonstrated that the majority of differentially expressed proteins were significantly enriched within cytoplasmic and membrane-bounded organelles. Notably, most proteins localized to vesicular compartments, while a substantial proportion were also associated with the extracellular region and the endomembrane system. Additional enrichment was observed in compartments related to secretory granules, the mucus layer, and lysosomal structures, reflecting disruption of vesicular trafficking, epithelial barrier regulation, and immune-related secretion. MF of GO analysis further demonstrated significant enrichment in carbohydrate binding and hydrolase activity acting on O-glycosyl compounds. Pathway enrichment analysis using Reactome identified significant representation of disease-related pathways, including general disease processes, disorders of metabolism, diseases of carbohydrate metabolism, innate immune signaling, immune system pathways, and neutrophil degranulation. In contrast, no statistically significant enrichment was observed in KEGG and WikiPathways analyses. The lack of significant KEGG and WikiPathways enrichment likely stems from database bias, as these libraries are primarily curated for intracellular signaling in classic tissues rather than the specialized mucosal-luminal interface of the fecal proteome. Many identified proteins are involved in extracellular defense and structural integrity, which do not cluster into canonical metabolic pathways, leading to statistical dilution in generalized enrichment tests (Chowdhury and Sarkar, 2015; Rowland et al., 2017). Utilizing STRING-based network analysis overcomes this limitation by detecting functional coherence through direct protein-protein interactions ($p < 0.05$) (Szklarczyk et al., 2023). Together, these findings show that the dysregulated proteins participate in metabolic, immune, and vesicle-associated pathways within the intestinal environment.

3.4. Protein–protein interaction and network mapping of differentially expressed proteins identified metabolic, immune and CFTR-related signaling in fluorosis

To investigate functional relationships among the 10 differentially expressed proteins, PPI analysis was performed using the STRING database (Fig. 4B). The resulting network revealed distinct functional interaction cluster related to immune activation and intestinal metabolism. C3 formed a discrete interaction cluster with three associated proteins linked to complement cascade activation and innate immune

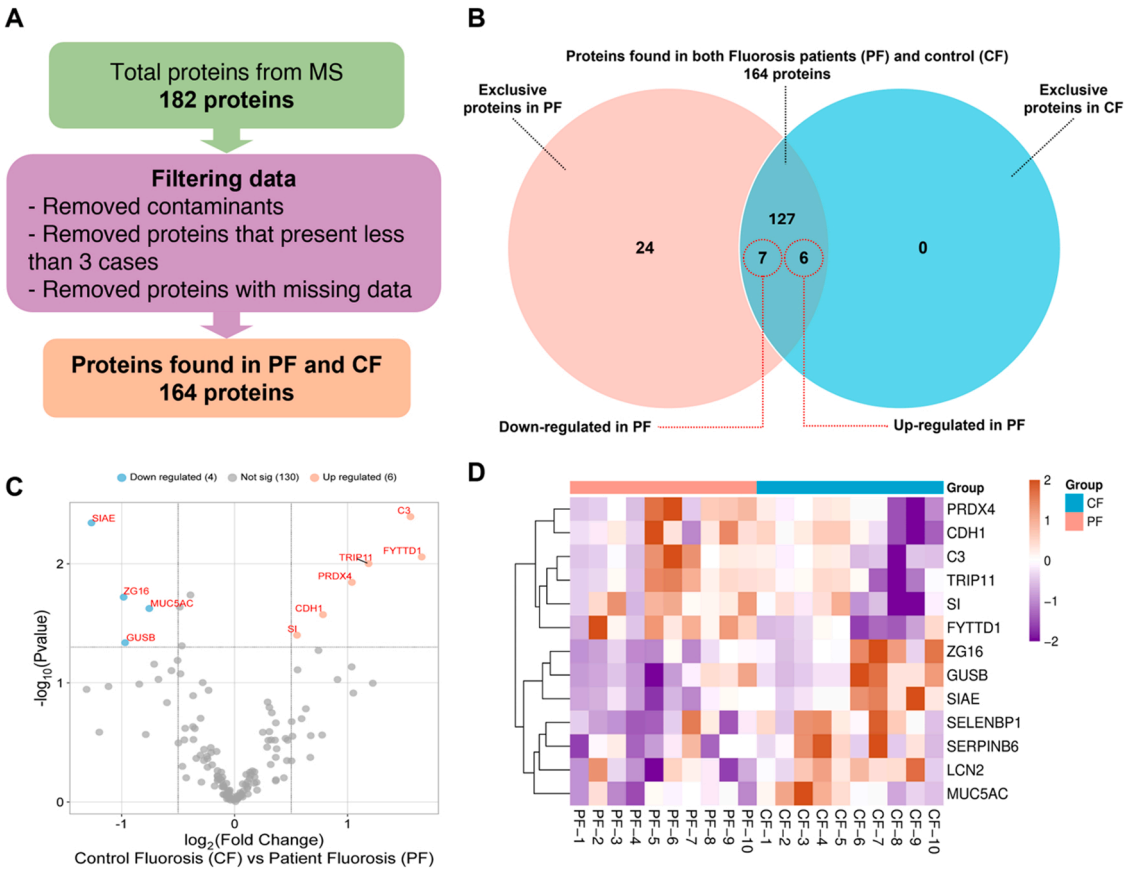

Fig. 2. Data filtering and proteomic analysis of fecal samples. (A) Flowchart outlining the data filtering and analysis steps. (B) Venn diagram showing the total number of identified proteins, proteins unique to the PF group, and significantly differentially expressed proteins (p-value < 0.05; $\log_2$ FC > 0.5 or < -0.5). (C) Volcano plot highlighting 13 significantly differentially expressed proteins, including 6 upregulated (pink) and 4 downregulated (blue), as well as 3 proteins with $|\log_2 FC| < 0.5$ that did not meet the fold-change threshold (gray). (D) Heatmap of hierarchical clustering showing distinct expression patterns of the 13 significantly differentially expressed proteins (p-value < 0.05) across the two groups. CF, control group (n = 10); PF, fluorosis patient group (n = 10).

Table 1
A list of 13 differentially expressed proteins found in both control and Fluorosis patients.

Genes	Accession	Description	Patients (log2)	Controls (log2)	p-value[a]	log2FC	FC
Up-regulated proteins (log2FC < −0.5 or log2FC > 0.5)							
C3	P01024	Complement C3	0.80	-0.75	0.004	1.56	2.94
FYTTD1	Q96QD9	UAP56-interacting factor	0.50	-1.16	0.009	1.66	3.15
TRIP11	Q15643	Thyroid receptor-interacting protein 11	0.39	-0.80	0.010	1.19	2.27
PRDX4	Q13162	Peroxiredoxin-4	0.30	-0.73	0.014	1.04	2.05
CDH1	P12830	Cadherin-1	-0.06	-0.84	0.027	0.78	1.72
SI	P14410	Sucrase-isomaltase, intestinal	0.28	-0.28	0.040	0.55	1.47
Down-regulated proteins (log2FC < −0.5 or log2FC > 0.5)							
SIAE	Q9HAT2	Sialate O-acetylesterase	-0.67	0.60	0.005	-1.27	0.42
ZG16	O60844	Zymogen granule membrane protein 16	-0.35	0.63	0.019	-0.98	0.51
MUC5AC	P98088	Mucin-5AC	-0.32	0.44	0.024	-0.76	0.59
GUSB	P08236	Beta-glucuronidase	0.00	0.97	0.046	-0.97	0.51
Proteins with low changes (log2FC > −0.5 or log2FC < 0.5)							
SELENBP1	Q13228–4	Isoform 4 of Methanethiol oxidase	0.05	0.44	0.018	-0.39	0.76
LCN2	P80188	Neutrophil gelatinase-associated lipocalin	-0.14	0.35	0.023	-0.49	0.71
SERPINB6	P35237	Serpin B6	-0.45	0.02	0.049	-0.47	0.72

[a] Differences between groups were analyzed using an independent t-test, with significance set at p-value < 0.05. Proteins exhibiting a $\log_2$ fold-change ($\log_2$FC) of either > 0.50 or < -0.50 were considered differentially expressed; FC; Fold-change.

responses. In parallel, MUC5AC, CDH1, ZG16, SI, GUSB, and SIAE were interconnected through a shared network of interaction partners, including MUC2, MUC15, KRT20, TFF3, CLCA1, GANC, and ARSB. Although FYTTD1, TRIP11, and PRDX4 did not exhibit direct interactions within the STRING core network, integration of the overall interaction landscape revealed convergence on two major functional axes: intestinal metabolic regulation, mediated largely through SI and GUSB, and immune regulation and innate defense, involving C3, CDH1, MUC5AC, PRDX4, and GUSB. Notably, STRING disease-association analysis mapping identified connections between several proteins to metabolic disorders (MUC5AC, SI, GUSB) and intestinal diseases (CDH1, SI).

To further refine protein network architecture, interaction analysis was extended using the IntAct database and visualized in Cytoscape

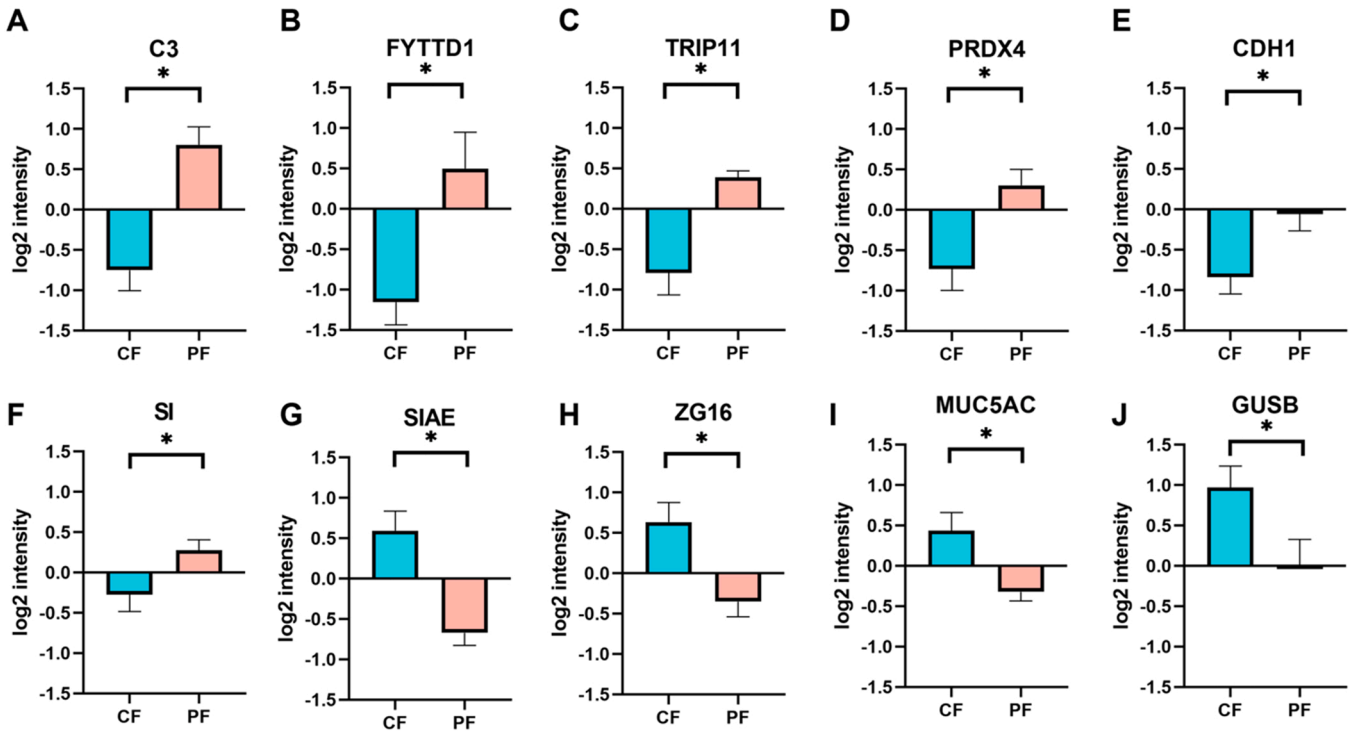

Fig. 3. Significantly altered proteins in PF groups. (A-F) Six significant upregulated proteins; (A) C3, (B) FYTTD1, (C) TRIP11, (D) PRDX4, (E) CDH1, and (F) SI. (G-J) Four significant downregulated proteins; (G) SIAE, (H) ZG16, (I) MUC5AC, and (J) GUSB.

(Fig. 4C). This analysis revealed that five upregulated proteins, C3, CDH1, PRDX4, FYTTD1, and TRIP11, were functionally linked to Cystic fibrosis transmembrane conductance regulator (CFTR), a key apical ion channel in intestinal epithelial cells. CDH1 formed a major interaction cluster centered on epithelial adhesion and cytoskeletal regulation, incorporating catenin beta 1 (CTNNB1), catenin delta 1 (CTNND1), serpin family H member 1 (SERPINH1 or Heat Shock Protein 47, HSP47), AKT serine/threonine kinase 1 (AKT1), fibroblast growth factor receptor 1 (FGFR1), epidermal growth factor receptor (EGFR), and actinin alpha 4 (ACTN4). A second interaction cluster was centered on PRDX4, which directly interacted with CFTR and formed a stress-response and transcriptional regulation network involving disulfide isomerase family A member 3 (PDIA3), collagen type I alpha 1 chain (COL1A1), jun proto-oncogene, AP-1 transcription factor subunit (JUN), superoxide dismutase 1 (SOD1), and estrogen receptor 1 and 2 (ESR1 and ESR2). TRIP11 exhibited direct interactions with FGFR family members (FGFR2, FGFR3, and FGFR4) as well as S100A9, while FYTTD1, a regulator of post-transcriptional RNA processing, interacted with chaperon protein nucleophosmin (NPM1) and was additionally connected to both CFTR and calcium voltage-gated channel subunit alpha1 C (CACNA1C). This interaction cluster further converged on C3, which interacted with FAM20C, a Golgi-associated secretory pathway kinase critically involved in biomineralization. Collectively, the PPI analyses reveal interconnected interaction clusters involving metabolic pathways, immune-related signaling, adhesion-associated proteins, and CFTR-linked regulatory components.

3.5. Functional and pathway annotation of fluorosis-specific fecal proteins

To further characterize the molecular features uniquely associated with fluorosis, the 24 proteins detected exclusively in the PF group (Supplementary Table S5) were subjected to functional annotation and enrichment analysis. GO enrichment and functional annotation analysis organized these proteins into 9 distinct functional clusters (Fig. 5A; Supplementary Table S6). The most significant functional enrichment was observed in pathways related to protease inhibition and immune regulation. Additional clusters were associated with epithelial integrity, cell adhesion, proliferation, and cytoskeletal organization. Several clusters were linked to protein folding, RNA binding, and cellular stress responses. Subcellular localization analysis demonstrated broad distribution across cytosolic, nuclear, membrane-associated, and extracellular compartments, with additional enrichment in plasma membrane–associated, secreted, and vesicle-related categories. Further functional clusters were related to actin cytoskeleton organization, contractile activity, and neuromuscular-associated processes. Overall, these analyses indicate that fluorosis-exclusive proteins participate in diverse biological and cellular pathways involving immune function, epithelial structure, stress responses, and cytoskeletal organization.

3.6. Protein–protein interaction and network analysis of fluorosis-exclusive proteins reveals CFTR-, integrin-, and metabolic regulator-centered signaling

Based on GO enrichment analysis of 24 proteins uniquely detected in PF group, the two most significant functional clusters, cluster 1 (serine protease–related processes) and cluster 2 (focal adhesion, cell proliferation–related processes), were selected for subsequent PPI and network analysis. The PPI network for Cluster 1 revealed a densely interconnected interaction cluster composed of fluorosis-exclusive proteins predominantly involved in serine protease inhibition, innate immune regulation, and antibacterial peptide responses (Fig. 5B). STRING analysis demonstrated extensive interactions among multiple protease inhibitor families, immune mediators, and epithelial defense proteins, highlighting a coordinated functional role in mucosal immune protection and inflammatory control. Within this network, SERPINB3, SERPINB4, SERPINB10, and SLPI emerged as central nodes, forming a tightly linked inhibitory interaction cluster regulating endopeptidase activity and antimicrobial peptide production. These interactions mapped directly onto the GO terms enriched in Cluster 1, including regulation of serine-type endopeptidase activity, innate immune responses, and antibacterial peptide production. Extended network analysis

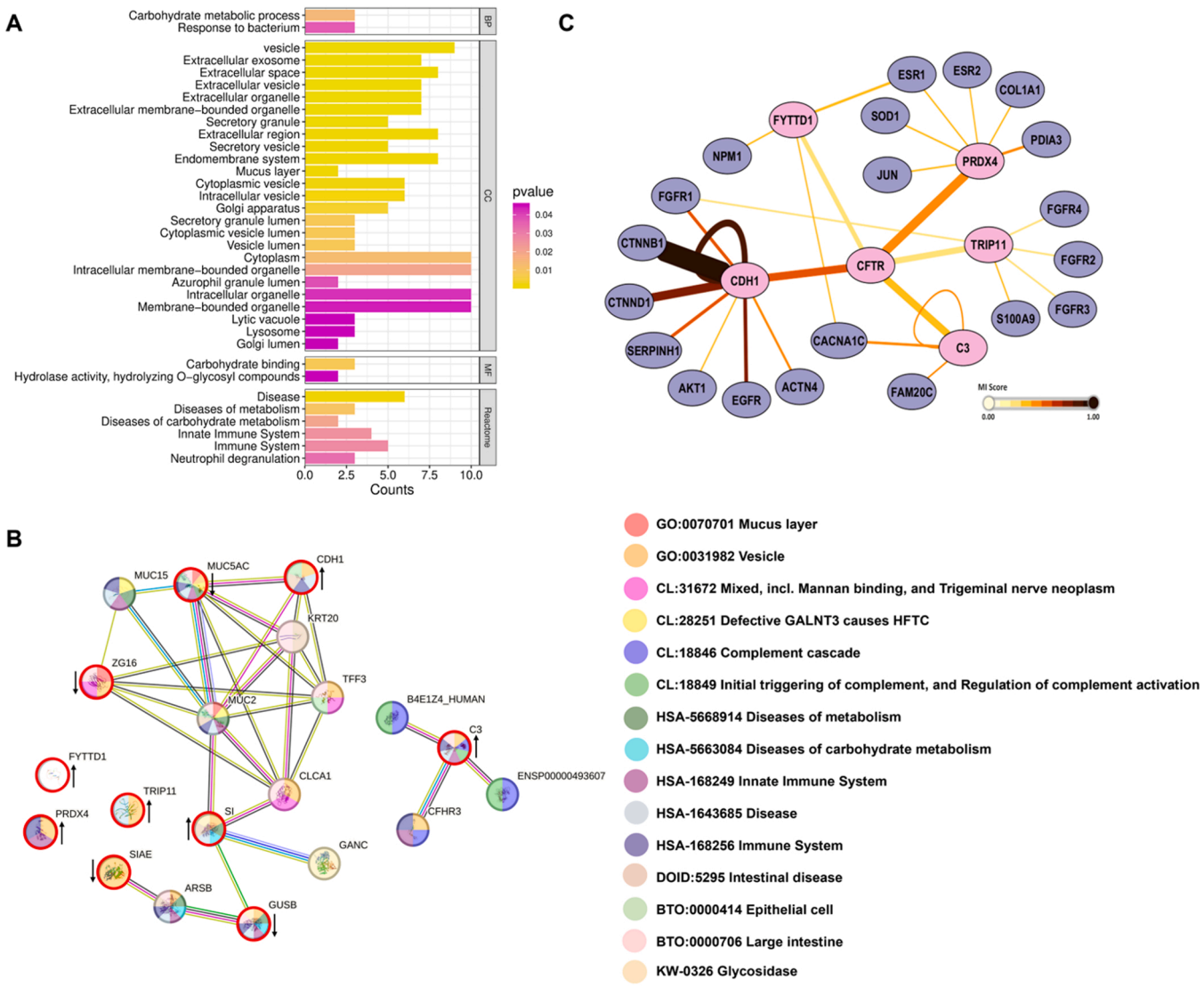

Fig. 4. Integrated metabolic, immune, and CFTR-associated networks revealed by fecal proteomic profiling in fluorosis. Differential fecal proteomic signatures between PF and CF were analyzed using GO, STRING, and PPI analyses. (A) GO and Reactome pathway enrichment indicate coordinated alterations in metabolic and immune-related processes, along with enrichment of intracellular trafficking-related cellular compartments. (B) STRING network analysis illustrates functional interrelationships among the 10 differentially expressed proteins, with core proteins shown in red circles. Arrows indicate up- and down-regulation. (C) IntAct-based PPI network visualized in Cytoscape highlights a CFTR-associated interaction cluster, with core proteins shown in pink circles and extended interaction partners shown in purple circles, indicating potential reorganization of intestinal-related pathways in fluorosis.

highlighted SERPINB3 as a major regulatory hub (Fig. 5C). SERPINB3 showed strong connectivity with innate immune signaling components, including CCR1, TNFRSF1B, IRAK4, BMX, MAP3K6, RNF115, and PIM1. Several Cluster 1 proteins also converged on CFTR. SERPINB3 and SERPINB10 demonstrated direct interactions with CFTR. Additional immune-associated proteins, including SLPI, ELANE, SRPK1, NFKBIB, and TRIM11, formed a secondary interaction cluster within the network.

The PPI of cluster 2 demonstrated direct interactions between multiple fluorosis-exclusive proteins, including FER, SERPINB3, PDIA3, NPM1, ACTN4, CALR, ACTB and TPM2 (Fig. 5D). The interaction pattern confirmed the functional enrichment observed in GO analysis, demonstrating strong associations with focal adhesion, actin cytoskeleton organization, and adherens junction components. A prominent feature of this network was the interaction of multiple Cluster 2 proteins with CFTR, which emerged as a central signaling hub (Fig. 5E), similar to the serine protease-related Cluster 1 network. Interestingly, MAPT emerged as a secondary hub sharing the same core interactors, reflecting a parallel interaction cluster related to cytoskeletal dynamics and cellular stress responses. Extended network mapping further identified bone morphogenetic proteins (BMP1 and BMP4), PDIA2, the ion transporter SLC26A4, and additional interacting proteins including SERPINH1, the signaling protein YWHAZ, COL1A1 and JUN, which connect to multiple core proteins within the CALR-centered hub. A second interaction cluster centered on PDIA3 exhibited broad connectivity with members of the integrin family (ITGB1, ITGA2, ITGA3, ITGB5, and ITGA6), annexin family proteins (ANXA4 and ANXA5), PRDX4, FGFR4, and STIM1, as well as SERPINH1, COL1A1, SERPINB3, SERPINB4, JUN and SOD1. Similar to the PDIA3-associated interaction cluster, ACTB is connected to members of the annexin family (ANXA1, ANXA2, and ANXA6), as well as FGFR1, ENO1, HSPA8 and ACTN2. In addition, ACTB was linked to ACTN4 via YWHAZ, EGFR, ESR1, and ESR2, and connected to SERPINB3 and NPM1 through MAP3K6 and through AKT1, JUN and EGFR, respectively. ACTN4 further interacted with CTNNB1 and CDH1, while indirect connections to NPM1 were mediated by ESR1, ESR2, VCAM1, FN1 and EGFR. The NPM1-centric interaction cluster further connected to a diverse set of proteins, including FYTTD1, NPM2,

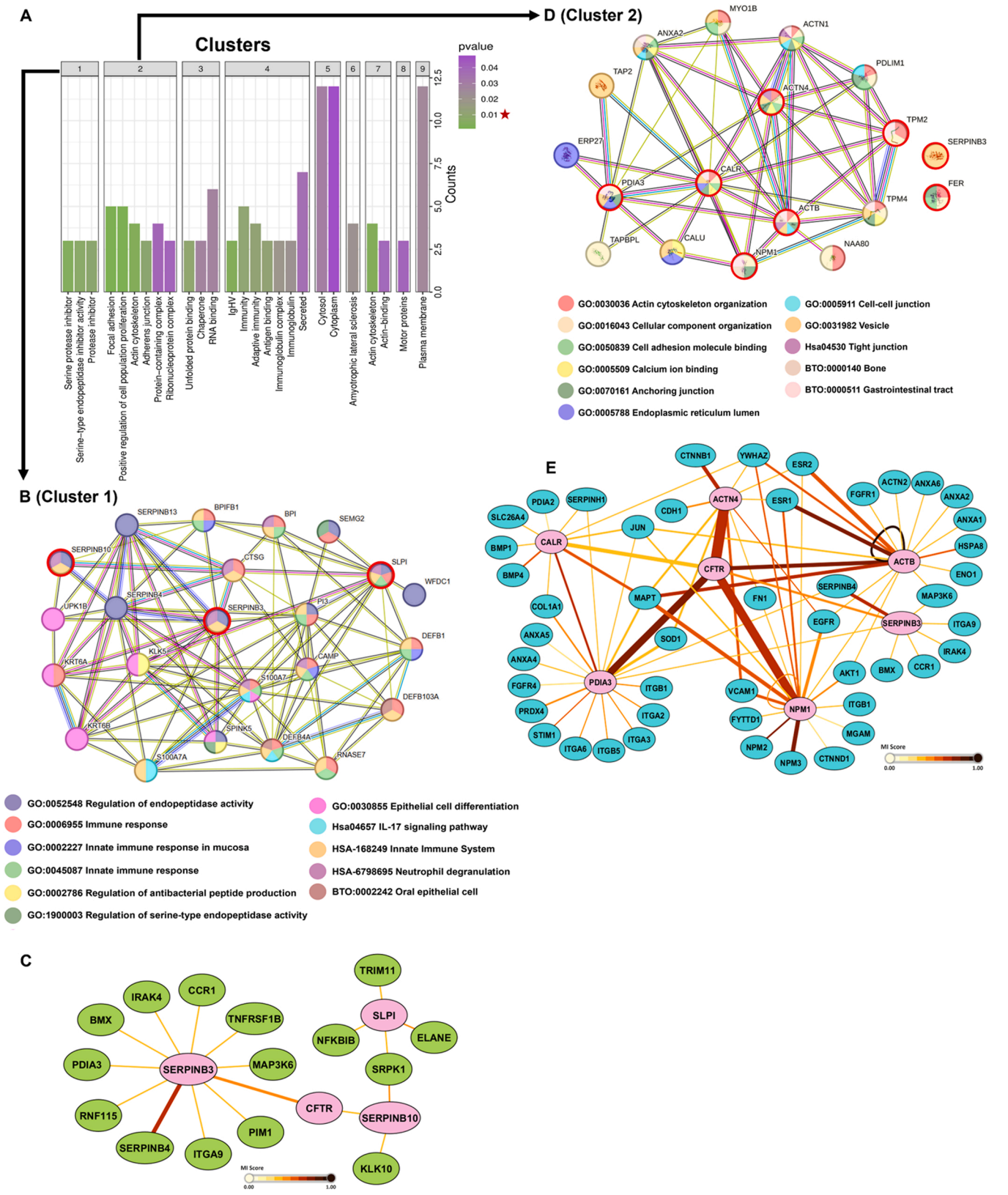

Fig. 5. PF-exclusive fecal proteins converge on immune, cytoskeletal, and CFTR-centered interaction networks. Integrated GO, STRING, and PPI analyses were applied to proteins exclusively detected in PF. (A) Clustered enrichment of GO and pathway annotations. Star indicate $p \leq 0.01$. (B) STRING network of 24 PF-exclusive proteins highlighting Cluster 1 enriched for immune-related functions. (C) IntAct-based PPI network visualized in Cytoscape corresponding to Cluster 1, revealing a densely connected immune-associated interaction cluster. (D) STRING network highlighting Cluster 2 associated with focal adhesion, adherens junctions, and cytoskeletal organization. (E) IntAct-based PPI network corresponding to Cluster 2 highlights a CFTR-centered interaction cluster. Across panels (C) and (E), core proteins are shown in pink circles, while extended interaction partners are shown in green (Cluster 1) or teal (Cluster 2).

NPM3, CTNND1, MGAM, and ITGB1, while the SERPINB3 interaction cluster appeared similar to Cluster 1. Overall, PPI mapping revealed that fluorosis-exclusive proteins form coordinated interaction networks related to protease regulation, immune-associated pathways, epithelial adhesion, cytoskeletal organization, and CFTR-linked signaling.

4. Discussion

In this study, we investigated host-derived molecular alterations associated with chronic fluoride exposure by profiling fecal proteins from school-aged children residing in a high-fluoride endemic area. Urinary fluoride measurements confirmed substantially elevated systemic exposure in children with fluorosis, establishing a clear exposure-response context for interpreting intestinal proteomic changes. The intestinal proteome demonstrated clear molecular stratification between fluorosis and control groups, revealing 10 significantly dysregulated proteins and 24 proteins exclusively detected in fluorosis patients. These signatures indicate that chronic fluoride exposure disrupts multiple biological systems, including epithelial adhesion, immune defense, vesicular trafficking, oxidative stress responses, and carbohydrate metabolism, reflecting the systemic nature of fluoride toxicity. Because fecal host proteins predominantly originate from epithelial turnover and mucosal secretions, the observed signatures most directly report altered mucosal homeostasis, particularly barrier injury/repair and immune activity, rather than intramucosal expression changes in isolation.

The upregulated proteins PRDX4, C3, CDH1, TRIP11, FYTTD1, and SI highlight a multifaceted epithelial and immune response. PRDX4, a key regulator of ER redox homeostasis (Elko et al., 2021; Fujii et al., 2025), points to activation of ER stress and oxidative defense pathways under fluoride toxicity (Aulestia et al., 2020). This response is consistent with extensive evidence showing that sustained fluoride exposure disrupts multiple organelles, including the mitochondria, ER, Golgi apparatus, and nucleus, leading to broad impairment of cellular homeostasis (Johnston and Strobel, 2020; Sharma et al., 2008; Wongong et al., 2024). *In vitro* studies further demonstrate that fluoride triggers profound ER stress, DNA fragmentation, cytoskeletal disruption, suppression of protein synthesis, reduced secretion of enamel matrix proteins, and ultimately apoptosis, illustrating the cascading cellular damage that accompanies chronic fluoride insult (Sharma et al., 2008; Wei et al., 2013). Upregulation of C3 indicates heightened activation of the complement system, a hallmark of innate immune stimulation that mirrors fluoride-associated intestinal inflammation and IBD-like phenotypes reported in experimental models (Wang et al., 2023). CDH1, a calcium-dependent transmembrane protein that mediates cell-cell adhesion through adherens junctions and barrier integrity (Lessey et al., 2022), together with cytoskeletal regulators identified among PF-exclusive proteins (ACTB, ACTN4), suggests that fluoride imposes structural strain on epithelial adhesion and barrier stability. TRIP11 and FYTTD1, regulators of Golgi organization and RNA processing, likely reflect adaptive responses to protein trafficking stress, aligning with the known effects of fluoride on the ER–Golgi axis (Kim et al., 2023; Williams et al., 2025; Yamaguchi et al., 2022). Increased SI expression, a brush-border disaccharidase involved in carbohydrate metabolism, may represent an epithelial attempt to maintain absorptive and metabolic function despite ongoing cellular stress (Gericke et al., 2017). These functional signatures, supported by GO enrichment in vesicle-associated compartments, carbohydrate metabolism, and immune pathways, reflect the multifaceted intestinal stress induced by fluoride.

Conversely, downregulated MUC5AC, ZG16, GUSB, and SIAE pointed toward impaired mucus barrier formation, weakened bacterial aggregation, disrupted lysosomal metabolism, and altered immune tolerance. MUC5AC, a major secreted mucin, is essential for maintaining the viscoelastic mucus barrier that prevents pathogen adherence and shields epithelial surfaces from mechanical and chemical injury (Rodríguez-Piñeiro et al., 2013). Reduced MUC5AC production weakens this first line of defense, decreasing mucus thickness and altering its biochemical properties, which can facilitate pathogen access, increase susceptibility to epithelial damage, and impair mucociliary-like clearance mechanisms within the gut (Hasnain et al., 2011; Rodríguez-Piñeiro et al., 2013). GUSB, a lysosomal hydrolase essential for glycosaminoglycan turnover and metabolic homeostasis, when decreased, may impair lysosomal function, disrupt autophagy, and compromise epithelial renewal (Grant et al., 2024). Reduced SIAE, a regulator of sialic acid–dependent immune tolerance, may lower the threshold for immune activation against commensal microbes, predisposing to inflammatory responses (Visser et al., 2021). ZG16 down-regulation is especially significant, as this bacterial-aggregating lectin normally limits microbial access to the epithelium. Its loss compromises this protective mechanism, destabilizes host–microbiota interactions, and promotes early inflammatory changes (Bergström et al., 2016; Chen et al., 2024). These downregulated proteins indicate weakened barrier integrity, altered lysosomal and immune processes, and reduced mucosal defense, molecular patterns consistent with the systemic nature of fluoride toxicity and its multi-organ manifestations.

Analysis of the 24 fluorosis-exclusive proteins revealed pronounced enrichment in pathways related to focal adhesion, actin cytoskeleton (Legerstee and Houtsmuller, 2021; Nowwarote et al., 2019), and adherens junction maintenance (Lessey et al., 2022), aligning with the up-regulation of CDH1. Within this network, ACTB emerged as a major structural hub coordinating cytoskeletal dynamics with broader regulatory programs. Its interactions connected cytoskeletal remodeling to growth factor signaling pathways (EGFR, FGFR1), which play essential roles in bone and tooth development (Linder et al., 2018; Pei et al., 2024; Porntaveetus et al., 2010), and to hormonal signaling via ESR1/ESR2, previously associated with bone metabolic disturbances and dental fluorosis (Dalledone et al., 2019). Notably, ACTB/PDIA3 networks intersected with calcium-dependent annexin pathways that are central to bone and tooth mineralization. These networks included annexin A family members, particularly ANXA1, ANXA2, ANXA5, and ANXA6, which regulate calcium binding, osteoblast and odontoblast differentiation, and extracellular matrix organization, thereby linking cytoskeletal dynamics to calcium-mediated mineralization processes (Xu et al., 2024). The presence of MAPT, a cytoskeletal-associated protein expressed in odontoblasts, further links this network to cytoskeletal organization in mineralizing cells (Miyazaki et al., 2015). The involvement of JUN, a downstream effector of the fluoride-responsive JNK/c-Jun pathway, further implicates these cytoskeletal interaction clusters in oxidative stress and enamel matrix dysregulation, consistent with evidence that JNK activation increases ROS and suppresses MMP20, impairing ameloblast function (kawasaki et al., 2014; Zhang et al., 2007). Other exclusive-protein clusters, particularly the PDIA3–CALR–SOD1 interaction cluster, highlight convergence on ER stress, protein folding, and redox homeostasis (Salati et al., 2019; Xu et al., 2022; Yoo et al., 2019). Together, the exclusive proteins reinforce a coherent model in which chronic fluoride exposure induces multilevel epithelial instability, integrating cytoskeletal remodeling with protease regulation, adhesion changes, and stress-adaptive mechanisms.

The proteomic landscape of dental fluorosis reveals a complex interplay between quantitative shifts in the existing proteome and the emergence of a qualitative biological switch. By analyzing both DEPs and fluorosis-exclusive proteins, we can characterize the host response as a dual-layered mechanism. While the DEPs reflect the adaptive modulation of homeostatic pathways, illustrating the specific degree of impairment in shared functions like epithelial barrier integrity, the presence of exclusive proteins points toward the activation of stress-induced *de novo* synthesis or the accelerated shedding of mucosal components that remain undetectable under baseline (Control) conditions. The emergence of this unique proteomic signature suggests that chronic fluoride exposure triggers a physiological state qualitatively distinct from the healthy homeostatic environment. Integrating both expression intensity and novel protein presence provides a comprehensive characterization of the stress-barrier-transport axis, offering a

clearer understanding of fluoride-induced intestinal disruption.

A prominent finding in this study was the emergence of CFTR as a central molecular hub linking several fluoride-responsive proteins. Multiple upregulated proteins, PRDX4, CDH1, TRIP11, FYTTD1, C3, and many fluorosis-exclusive proteins converged on CFTR within the interaction networks, indicating that ion transport and epithelial barrier regulation are key nodes of fluoride-induced stress. In the mucosal surfaces of the mouth and gut, this initial imbalance triggers tissue-specific responses, such as metabolic reprogramming (e.g., LDHA) in saliva and a breakdown of the immune-epithelial barrier in the intestines. In our data, PRDX4 acts as a specialized node within the CFTR-associated stress cluster, indicating a targeted antioxidant response to the redox imbalance caused by disrupted transport. Similarly, the dysregulation of MUC5AC and CDH1 is directly linked to the structural reconfiguration of the intestinal barrier identified in our PPI maps. These findings align with recent salivary proteomic data from fluorosis patients, where CFTR-associated pathways were identified as potential contributors to enamel pathology (Gavila et al., 2024; Pumchan et al., 2026). Notably, CFTR dysfunction is known to increase mucus viscosity and alter inflammatory signaling (Pawłowska et al., 2025) paralleling the proteomic signatures of mucosal instability and immune activation observed in this study. Eventually, these localized soft-tissue stresses converge into a broader systemic effect, as seen in urinary proteomic data where mucosal impairment aligns with signs of damaged matrix integrity and abnormal biomineralization (e.g., SPP1 and TNC; (Pongsapipatana et al., 2026)). Together, these data provide a unified molecular framework explaining how fluoride-induced transport stress drives the systemic manifestations of dental and skeletal fluorosis.

Connections between intestinal interaction networks and biomineralization pathways further emphasize the multisystem consequences of fluoride toxicity. The association of C3 with FAM20C, alongside CACNA1C, major voltage-dependent calcium channel, suggests that fluoride-induced epithelial and immune stress may intersect directly with regulatory pathways essential for enamel and skeletal mineralization (Baker et al., 2025; Nitayavardhana et al., 2020; Nurbaeva et al., 2017). Because CACNA1C governs calcium influx, its co-occurrence within the same interaction landscape as CFTR and C3 implies that fluoride disrupts not only ion transport but also calcium homeostasis, a core determinant of both immune activation and mineralized tissue formation. Calcium signaling orchestrates key immune functions, including lymphocyte proliferation, differentiation, and activation (Ingale et al., 2024), and perturbations in intracellular Ca^{2+} can impair CFTR trafficking and channel stability-mechanisms implicated in the development of dental fluorosis (Billet and Hanrahan, 2013; Duan, 2014; Gupta et al., 2025). Given the established roles of FAM20A/FAM20C in tooth and bone development, and the dependency of osteoblast and ameloblast function on calcium deposition (Sriwattanapong et al., 2025, 2024), these interactions provide a mechanistic bridge linking intestinal perturbations to both dental fluorosis and skeletal fluorosis. This mechanistic link is further supported by recent urinary proteomic evidence from children exposed to high fluoride levels, which identified coordinated interactions among SPP1, TNC, FAM20A, and FAM20C, defining a regulatory axis linking extracellular matrix organization, phosphate homeostasis, and bone mineralization (Pongsapipatana et al., 2026). Collectively, these findings suggest that fluoride-induced disturbances in intestinal ion transport, calcium signaling, immune regulation, and epithelial barrier function converge on FAM20A/FAM20C-dependent mineralization pathways, potentially amplifying defects in skeletal homeostasis and underscoring the gut as a critical mediator of systemic fluorosis pathophysiology.

Fluoride's effects extended beyond host-derived proteins and are consistent with microbiome alterations reported in human and animal studies (Bibi et al., 2024; Li et al., 2021; Qiu et al., 2020; Wang et al., 2023; Zhong et al., 2022; Zhou et al., 2023; Zhu et al., 2022). Previous studies have shown that excessive fluoride exposure induces reproducible shifts in gut microbial composition (Zhou et al., 2023), including depletion of beneficial SCFA-producing taxa (*Lactobacillus, Faecalibacterium,* and *Bacteroidetes*) and enrichment of Proteobacteria, a hallmark of epithelial stress and dysbiosis (Chen et al., 2021; Rawat et al., 2025). This excess fluoride promotes dysbiosis, diminished SCFA production, and impaired host–microbiota symbiosis, thereby increasing susceptibility to intestinal inflammation, IBD, colitis, and colorectal cancer (Bibi et al., 2024; Dionizio et al., 2021; Zhu et al., 2022). Fluoride exerts a biphasic effect on gut diversity, with high doses triggering a sharp increase in taxa such as *Pelagibacterium, Unclassified Ruminococcaceae, and Unclassified Bdellovibrionales*, all of which correlates directly with the severity of dental fluorosis (Zhong et al., 2022). Proteobacterial shift mirrors findings in the oral microbiome of fluorosis patients, where *Neisseria* species (*N. sicca*, *N. cinerea*) were the most enriched (Ajrithirong et al., 2025). Consistent with these findings, our proteomic observations, specifically the downregulation of ZG16, MUC5AC, SIAE, and GUSB, serve as a biological mirror to these reported microbial disruptions. By compromising proteins essential for epithelial adhesion, mucus integrity, and bacterial aggregation, fluoride exposure appears to weaken the host-derived defenses necessary to maintain a healthy microbial balance. When these protective barriers are diminished, it facilitates the shift toward the dysbiotic environment and pro-inflammatory state associated with excessive fluoride intake.

This study offers molecular insight into fluoride-associated biological alterations but has

several limitations. The sample size was relatively small; however, all participants were age-matched children residing in the same high-fluoride endemic region in Ratchaburi Province, Thailand during a period of tooth development, which specific focus minimized environmental variability and allowed for a highly controlled investigation and makes the cohort highly suitable for this discovery-oriented investigation. We utilized a phenotypic extremes approach (TF0 vs. TF5–9) to maximize the signal-to-noise ratio; however, the lack of a moderate fluorosis gradient (TF1–4) prevents the identification of a specific tipping point or a linear dose-response relationship for intestinal dysregulation. Furthermore, while the 164 host proteins identified provide a biologically coherent snapshot, the protease-rich nature of the fecal matrix may have limited the detection of low-abundance proteins, and restricted sample volumes precluded targeted independent validation (e.g., Western blot) for key hubs like CFTR and MUC5AC. It is also important to note that fecal proteomics reflects a biological mirror of the mucosal-luminal interface, capturing epithelial shedding and mucosal secretion, rather than direct intracellular expression within the intact mucosa (Harder et al., 2024; Neurath et al., 2025). Finally, a key limitation is the absence of direct clinical indicators for intestinal permeability (e.g., lactulose/mannitol assays) or systemic inflammatory markers (e.g., CRP, IL-6). While 24-hour urinary fluoride was utilized as a gold-standard indicator of current systemic burden (Bennekou et al., 2025), the lack of corresponding clinical phenotypes means these proteomic shifts should be interpreted as candidate molecular signatures. In pediatric research, prioritizing non-invasive discovery is an ethical necessity; however, future longitudinal and multi-center studies, incorporating direct clinical measures of gut health and inflammatory status, are essential to confirm the geographic generalizability of these findings and to definitively establish the functional value of these proteins as biomarkers for fluoride-induced intestinal injury.

In conclusion, this discovery-phase study demonstrates that chronic childhood fluoride exposure is associated with a coordinated disruption of epithelial, immune, and metabolic pathways, supporting a systems-level view of fluorosis that extends beyond enamel formation. Our data suggest a fluoride-induced epithelial stress model, where knowledge-based interaction mapping identifies a CFTR-centered ion-transport and barrier-regulation axis as a key convergence point for fluoride-induced dysregulation. Specifically, the emergence of hubs involving oxidative stress and mucosal integrity suggests a molecular transition from systemic fluoride exposure to localized intestinal impairment (Fig. 6). These proteomic shifts indicate compromised

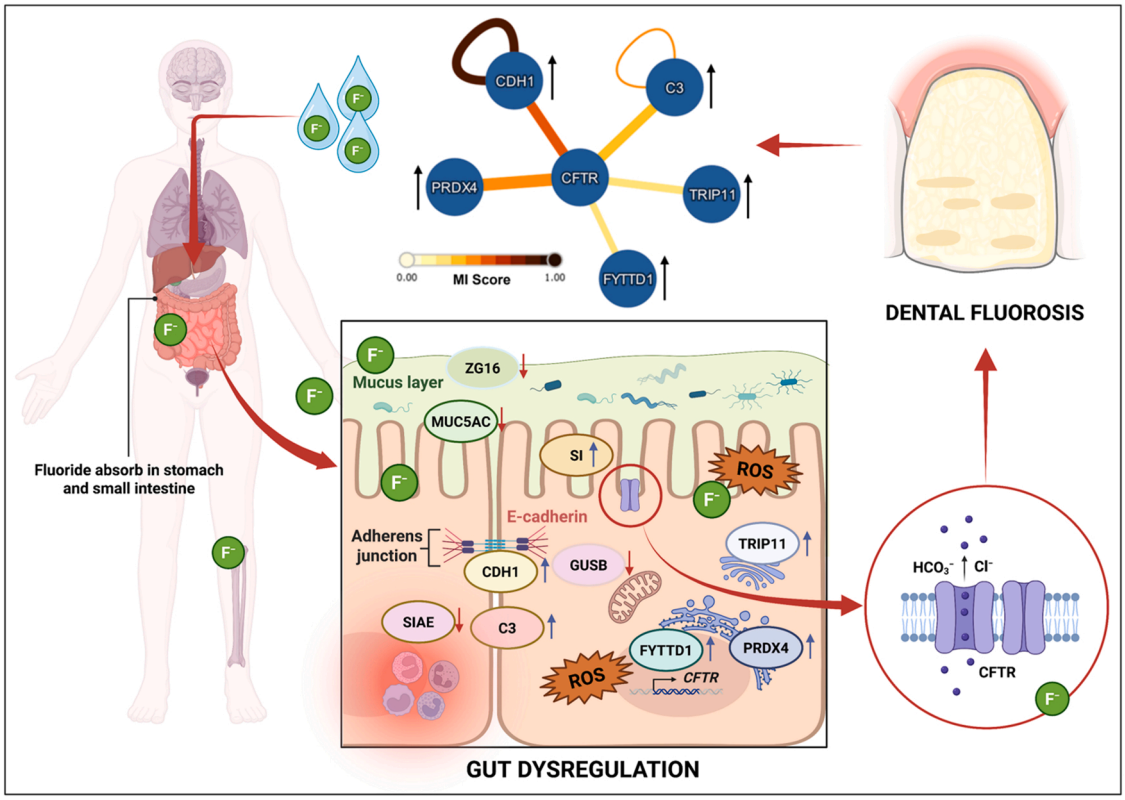

Fig. 6. Impact of high fluoride exposure on systemic health linking gut dysregulation to dental fluorosis. Schematic overview illustrates the proposed relationship between chronic fluoride exposure, intestinal molecular alterations, and dental outcomes. Fluoride intake leads to accumulation in the gastrointestinal tract, where alterations in the mucus layer, epithelial integrity, immune-related proteins, oxidative stress responses, and vesicle trafficking are observed. Network analysis highlights a CFTR-centered interaction cluster connecting redox regulation (PRDX4), protein trafficking (FYTTD1, TRIP11), complement signaling (C3), and adherens junction components (CDH1/E-cadherin). These intestinal molecular perturbations are proposed to influence systemic fluoride handling and downstream effects on dental tissues, contributing to the development of dental fluorosis.

mucus integrity and altered mucosal-luminal homeostasis, patterns that align with the systemic manifestations seen in endemic fluorosis. As a foundational framework in an endemic pediatric population, this work nominates CFTR dysfunction as a potential systemic node linking intestinal perturbations to broader biomineralization defects. Future longitudinal studies and independent protein validation should be essential to define the full biological consequences of chronic fluoride exposure and the causal mechanisms driving these multi-system alterations.

CRediT authorship contribution statement

Kanokwan Sriwattanapong: Writing – review & editing, Validation, Supervision, Resources, Project administration, Methodology, Investigation, Funding acquisition, Data curation, Conceptualization. **Thantrira Porntaveetus:** Writing – review & editing, Validation, Supervision, Resources, Project administration, Methodology, Investigation, Funding acquisition, Data curation, Conceptualization. **Thutchima Khieota:** Writing – review & editing, Investigation. **Han-Sung Jung:** Writing – review & editing. **Hamid Alinejad-Rokny:** Writing – review & editing, Formal analysis. **Sung-Dae Cho:** Writing – review & editing. **Nawapan Pongsapipatana:** Writing – review & editing, Writing – original draft, Visualization, Validation, Formal analysis, Conceptualization. **Patcharaporn Gavila:** Writing – review & editing, Investigation.

Declaration of Competing Interest

The authors declare that they have no known competing financial interests or personal relationships that could have appeared to influence the work reported in this paper.

Acknowledgements

This research project is supported by the Second Century Fund (C2F), Chulalongkorn University, Thailand. KS was supported by the Faculty of Dentistry (DRF 68_006), the Ratchadaphiseksomphot Endowment Fund, Chulalongkorn University (grants for development of new faculty staff; DNS_67_042_3200_002 and The Exchange Faculty Travel Grant; Grant No. CTG168039), and Thailand Science Research and Innovation Fund Chulalongkorn University (HEA_FF_69_051_3200_004). TP was supported by the Ratchadaphiseksomphot Endowment Fund, Chulalongkorn University (The Exchange Faculty Travel Grant; Grant No. CTG168027).

Appendix A. Supporting information

Supplementary data associated with this article can be found in the online version at doi:10.1016/j.ecoenv.2026.120310.

Data availability

Data is provided within the manuscript or supplementary information files

References

Agrawal, A., Balcı, H., Hanspers, K., Coort, S.L., Martens, M., Slenter, D.N., Ehrhart, F., Digles, D., Waagmeester, A., Wassink, I., Abbassi-Daloii, T., Lopes, E.N., Iyer, A., Acosta, Javier M., Willighagen, L.G., Nishida, K., Riutta, A., Basaric, H., Evelo, Chris T., Pico, Alexander R., 2023. WikiPathways 2024: next generation pathway database. Nucleic Acids Res. 52 (D1), D679–D689. https://doi.org/10.1093/nar/gkad960.

Ajrithirong, P., Krasaesin, A., Sriarj, W., Gavila, P., Chetruengchai, W., Sriwattanapong, K., Manaspon, C., Samaranayake, L., Porntaveetus, T., 2025. The metagenome and metabolome signatures of dental biofilms associated with severe dental fluorosis. J. Oral. Microbiol. 17 (1), 2560591. https://doi.org/10.1080/20002297.2025.2560591.

Amadeu de Oliveira, F., MacVinish, L.J., Amin, S., Herath, D., Jeggle, P., Mela, I., Pieri, M., Sharma, C., Jarvis, G.E., Levy, F.M., Santesso, M.R., Khan, Z.N., Leite, A.L., Oliveira, R.C., Buzalaf, M.A.R., Edwardson, J.M., 2018. The effect of fluoride on the structure, function, and proteome of intestinal epithelia. Environ. Toxicol. 33 (1), 63–71. https://doi.org/10.1002/tox.22495.

Aulestia, F.J., Groeling, J., Bomfim, G.H.S., Costiniti, V., Manikandan, V., Chaloemtoem, A., Concepcion, A.R., Li, Y., Wagner, L.E., Idaghdour, Y., Yule, D.I., Lacruz, R.S., 2020. Fluoride exposure alters Ca^{2+} signaling and mitochondrial function in enamel cells. Sci. Signal 13 (619), eaay0086. https://doi.org/10.1126/scisignal.aay0086.

Baker, A., Al Tarrass, M., Chatziantoniou, C., Kozyraki, R., 2025. FAM20C and FAM20A in normal and ectopic mineralization: a focus on oro-renal syndromes. Matrix Biol. 142, 58–85. https://doi.org/10.1016/j.matbio.2025.11.002.

Bennekou, S.H., Allende, A., Bearth, A., Casacuberta, J., Castle, L., Coja, T., Crépet, A., Hoogenboom, R., Knutsen, H., Lambré, C., Nielsen, S.S., Turck, D., Civera, A.V., Villa, R., Zorn, H., Castenmiller, J., Cheyns, K., Darney, K., Gilbert, M., Halldorsson, T., 2025. Updated consumer risk assessment of fluoride in food and drinking water including the contribution from other sources of oral exposure. Efsa J. 23 (7), e9478. https://doi.org/10.2903/j.efsa.2025.9478.

Bergström, J.H., Birchenough, G.M., Katona, G., Schroeder, B.O., Schütte, A., Ermund, A., Johansson, M.E., Hansson, G.C., 2016. Gram-positive bacteria are held at a distance in the colon mucus by the lectin-like protein ZG16. Proc. Natl. Acad. Sci. USA 113 (48), 13833–13838. https://doi.org/10.1073/pnas.1611400113.

Bibi, S., Kerbiriou, C., Uzma, McKirdy, S., Kostrytsia, A., Rasheed, H., Eqani, S.A.M.A.S., Gerasimidis, K., Nurulain, S.M., Ijaz, U.Z., 2024. Gut microbiome and function are altered for individuals living in high fluoride concentration areas in Pakistan. Ecotoxicol. Environ. Saf. 284, 116959. https://doi.org/10.1016/j.ecoenv.2024.116959.

Billet, A., Hanrahan, J.W., 2013. The secret life of CFTR as a calcium-activated chloride channel. J. Physiol. 591 (21), 5273–5278. https://doi.org/10.1113/jphysiol.2013.261909.

Bronckers, A.L., Lyaruu, D.M., DenBesten, P.K., 2009. The impact of fluoride on ameloblasts and the mechanisms of enamel fluorosis. J. Dent. Res. 88 (10), 877–893. https://doi.org/10.1177/0022034509343280.

Chen, G., Hu, P., Xu, Z., Peng, C., Wang, Y., Wan, X., Cai, H., 2021. The beneficial or detrimental fluoride to gut microbiota depends on its dosages. Ecotoxicol. Environ. Saf. 209, 111732. https://doi.org/10.1016/j.ecoenv.2020.111732.

Chen, X., Chen, Y., Zhang, Y., Zhang, Y., Wang, Y., Li, Y., Sun, Y., Meng, G., Yang, G., Li, H., 2024. ZG16 impacts gut microbiota-associated intestinal inflammation and pulmonary mucosal function through bacterial metabolites. Int. Immunopharmacol. 141, 112995. https://doi.org/10.1016/j.intimp.2024.112995.

Chowdhury, S., Sarkar, R.R., 2015. Comparison of human cell signaling pathway databases–evolution, drawbacks and challenges. Database 2015. https://doi.org/10.1093/database/bau126.

Chuah, C.J., Lye, H.R., Ziegler, A.D., Wood, S.H., Kongpun, C., Rajchagool, S., 2016. Fluoride: A naturally-occurring health hazard in drinking-water resources of Northern Thailand. Sci. Total Environ. 545-546, 266–279. https://doi.org/10.1016/j.scitotenv.2015.12.069.

Dalledone, M., Cunha, A.S., Ramazzotto, L.A., Pecharki, G.D., Nelson-Filho, P., Scariot, R., Trevilatto, P.C., Vieira, A.R., Küchler, E.C., Brancher, J.A., 2019. Estrogen receptor gene is associated with dental fluorosis in Brazilian children. Clin. Oral. Invest. 23 (9), 3565–3570. https://doi.org/10.1007/s00784-018-2778-2.

Dec, K., Łukomska, A., Maciejewska, D., Jakubczyk, K., Baranowska-Bosiacka, I., Chlubek, D., Wąsik, A., Gutowska, I., 2017. The influence of fluorine on the disturbances of homeostasis in the central nervous system. Biol. Trace Elem. Res. 177 (2), 224–234. https://doi.org/10.1007/s12011-016-0871-4.

Dionizio, A., Uyghurturk, D.A., Melo, C.G.S., Sabino-Arias, I.T., Araujo, T.T., Ventura, T. M.S., Perles, J.V.C.M., Zanoni, J.N., Den Besten, P., Buzalaf, M.A.R., 2021. Intestinal changes associated with fluoride exposure in rats: Integrative morphological, proteomic and microbiome analyses. Chemosphere 273, 129607. https://doi.org/10.1016/j.chemosphere.2021.129607.

Dionizio, A.S., Melo, C.G.S., Sabino-Arias, I.T., Ventura, T.M.S., Leite, A.L., Souza, S.R.G., Santos, E.X., Heubel, A.D., Souza, J.G., Perles, J.V.C.M., Zanoni, J.N., Buzalaf, M.A. R., 2018. Chronic treatment with fluoride affects the jejunum: insights from proteomics and enteric innervation analysis. Sci. Rep. 8 (1), 3180. https://doi.org/10.1038/s41598-018-21533-4.

Duan, X., 2014. Ion channels, channelopathies, and tooth formation. J. Dent. Res 93 (2), 117–125. https://doi.org/10.1177/0022034513507066.

Elko, E.A., Manuel, A.M., White, S., Zito, E., van der Vliet, A., Anathy, V., Janssen-Heininger, Y.M.W., 2021. Oxidation of peroxiredoxin-4 induces oligomerization and promotes interaction with proteins governing protein folding and endoplasmic reticulum stress. J. Biol. Chem. 296, 100665. https://doi.org/10.1016/j.jbc.2021.100665.

Fujii, J., Ochi, H., Yamada, S., 2025. A comprehensive review of peroxiredoxin 4, a redox protein evolved in oxidative protein folding coupled with hydrogen peroxide detoxification. J. Free Radic. Biol. Med. 227, 336–354. https://doi.org/10.1016/j.freeradbiomed.2024.12.015.

Gavila, P., Ajrithirong, P., Chumnanprai, S., Kalpongnukul, N., Pisitkun, T., Chantarangsu, S., Sriwattanapong, K., Tagami, J., Porntaveetus, T., 2024. Salivary proteomic signatures in severe dental fluorosis. Sci. Rep. 14, 18372. https://doi.org/10.1038/s41598-024-69409-0.

Gericke, B., Schecker, N., Amiri, M., Naim, H.Y., 2017. Structure-function analysis of human sucrase-isomaltase identifies key residues required for catalytic activity. J. Biol. Chem. 292 (26), 11070–11078. https://doi.org/10.1074/jbc.M117.791939.

Grant, C.L., López-Valdez, J., Marsden, D., Ezgü, F., 2024. Mucopolysaccharidosis type VII (Sly syndrome) - What do we know? Mol. Genet Metab. 141 (3), 108145. https://doi.org/10.1016/j.ymgme.2024.108145.

Gupta, U., Tripathi, S., Bj, S., Mishra, S., 2025. Fluoride exposure and toxicity: comprehensive review of health risks and prevention. J. Neonatal Surg. 14 (4S), 1376–1389. ⟨https://www.jneonatalsurg.com/index.php/jns/article/view/7691⟩.

Harder, B.J., Lekkerkerker, A.N., Casavant, E.P., Hackney, J.A., Nguyen, A., McBride, J. M., Mathews, W.R., Anania, V.G., 2024. Comprehensive profiling of the human fecal proteome from IBD patients with DIA-MS enables evaluation of disease-relevant proteins. Proteom. Clin. Appl. 18 (5), e2300075. https://doi.org/10.1002/prca.202300075.

Hasnain, S.Z., Evans, C.M., Roy, M., Gallagher, A.L., Kindrachuk, K.N., Barron, L., Dickey, B.F., Wilson, M.S., Wynn, T.A., Grencis, R.K., Thornton, D.J., 2011. Muc5ac: a critical component mediating the rejection of enteric nematodes. J. Exp. Med. 208 (5), 893–900. https://doi.org/10.1084/jem.20102057.

Ingale, S., Rathored, J., Shende, S., Wankhade, S., 2024. The role of calcium homeostasis in modulating the immune response in cancer and infectious diseases. Multidiscip. Rev. 8, 2025034. https://doi.org/10.31893/multirev.2025034.

Johnston, N.R., Strobel, S.A., 2020. Principles of fluoride toxicity and the cellular response: a review. Arch. Toxicol. 94 (4), 1051–1069. https://doi.org/10.1007/s00204-020-02687-5.

Kanehisa, M., Furumichi, M., Sato, Y., Kawashima, M., Ishiguro-Watanabe, M., 2023. KEGG for taxonomy-based analysis of pathways and genomes. Nucleic Acids Res. 51 (D1), D587–d592. https://doi.org/10.1093/nar/gkac963.

kawasaki, M., Porntaveetus, T., Kawasaki, K., Oommen, S., Otsuka-Tanaka, Y., Hishinuma, M., Nomoto, T., Maeda, T., Takubo, K., Suda, T., Sharpe, P.T., Ohazama, A., 2014. R-spondins/Lgrs expression in tooth development. Dev. Dyn. 243 (6), 844–851. https://doi.org/10.1002/dvdy.24124.

Kim, J.A., Vetrivel, P., Kim, S.M., Ha, S.E., Kim, H.H., Bhosale, P.B., Heo, J.D., Lee, W.S., Senthil, K., Kim, G.S., 2021. Quantitative proteomics analysis for the identification of differential protein expression in calf muscles between young and old SD rats using mass spectrometry. ACS Omega 6 (11), 7422–7433. https://doi.org/10.1021/acsomega.0c05821.

Kim, W.K., Choi, W., Deshar, B., Kang, S., Kim, J., 2023. Golgi stress response: new insights into the pathogenesis and therapeutic targets of human diseases. Mol. Cells 46 (4), 191–199. https://doi.org/10.14348/molcells.2023.2152.

Legerstee, K., Houtsmuller, A.B., 2021. A layered view on focal adhesions. Biology 10 (11), 1189. https://doi.org/10.3390/biology10111189.

Lessey, L.R., Robinson, S.C., Chaudhary, R., Daniel, J.M., 2022. Adherens junction proteins on the move-From the membrane to the nucleus in intestinal diseases. Front Cell Dev. Biol. 10, 998373. https://doi.org/10.3389/fcell.2022.998373.

Li, A., Wang, Y., He, Y., Liu, B., Iqbal, M., Mehmood, K., Jamil, T., Chang, Y., Hu, L., Li, Y., Guo, J., Pan, J., Tang, Z., Zhang, H., 2021. Environmental fluoride exposure disrupts the intestinal structure and gut microbial composition in ducks. Chemosphere 277, 130222. https://doi.org/10.1016/j.chemosphere.2021.130222.

Linder, M., Hecking, M., Glitzner, E., Zwerina, K., Holcmann, M., Bakiri, L., Ruocco, M. G., Tuckermann, J., Schett, G., Wagner, E.F., Sibilia, M., 2018. EGFR controls bone development by negatively regulating mTOR-signaling during osteoblast differentiation. Cell Death Differ. 25 (6), 1094–1106. https://doi.org/10.1038/s41418-017-0054-7.

Liu, J., Zhao, J., Zhang, Y., Zhang, C., Yang, G., Tian, W., Zhou, B., Wang, H., 2025. Underlying Mechanism of Fluoride Inhibits Colonic Gland Cells Proliferation by Inducing an Inflammation Response. Biol. Trace Elem. Res 203 (2), 973–985. https://doi.org/10.1007/s12011-024-04212-6.

Makjaroen, J., Somparn, P., Hodge, K., Poomipak, W., Hirankarn, N., Pisitkun, T., 2018. Comprehensive Proteomics Identification of IFN-λ3-regulated Antiviral Proteins in HBV-transfected Cells. Mol. Cell Proteom. 17 (11), 2197–2215. https://doi.org/10.1074/mcp.RA118.000735.

McGrady, M.G., Ellwood, R.P., Srisilapanan, P., Korwanich, N., Worthington, H.V., Pretty, I.A., 2012. Dental fluorosis in populations from Chiang Mai, Thailand with different fluoride exposures - paper 1: assessing fluorosis risk, predictors of fluorosis and the potential role of food preparation. BMC Oral. Health 12, 16. https://doi.org/10.1186/1472-6831-12-16.

McGrady, M.G., Ellwood, R.P., Srisilapanan, P., Korwanich, N., Taylor, A., Goodwin, M., Pretty, I.A., 2012. Dental fluorosis in populations from Chiang Mai, Thailand with different fluoride exposures - paper 2: the ability of fluorescence imaging to detect differences in fluorosis prevalence and severity for different fluoride intakes from water. BMC Oral. Health 12, 33. https://doi.org/10.1186/1472-6831-12-33.

Melo, C.G.S., Perles, J., Zanoni, J.N., Souza, S.R.G., Santos, E.X., Leite, A.L., Heubel, A.D., CO, E.S., Souza, J.G., Buzalaf, M.A.R., 2017. Enteric innervation combined with proteomics for the evaluation of the effects of chronic fluoride exposure on the duodenum of rats. Sci. Rep. 7 (1), 1070. https://doi.org/10.1038/s41598-017-01090-y.

Milacic, M., Beavers, D., Conley, P., Gong, C., Gillespie, M., Griss, J., Haw, R., Jassal, B., Matthews, L., May, B., Petryszak, R., Ragueneau, E., Rothfels, K., Sevilla, C., Shamovsky, V., Stephan, R., Tiwari, K., Varusai, T., Weiser, J., D'Eustachio, P., 2023. The Reactome Pathway Knowledgebase 2024. Nucleic Acids Res. 52 (D1), D672–D678. https://doi.org/10.1093/nar/gkad1025.

Miyazaki, T., Baba, T.T., Mori, M., Moriishi, T., Komori, T., 2015. Microtubule-associated protein tau (Mapt) is expressed in terminally differentiated odontoblasts and severely down-regulated in morphologically disturbed odontoblasts of Runx2 transgenic mice. Cell Tissue Res 361 (2), 457–466. https://doi.org/10.1007/s00441-015-2135-6.

Naghavi, M., Kyu, H.H., Bhoomadevi, A., Aalipour, M.A., Aalruz, H., Ababneh, H.S., Abafita, B.J., Abaraogu, U.O., Abbafati, C., Abbasi, M., Abbaspour, F., Abbastabar, H., Abd Al Magied, A.H.A., Elhafeez, S.A., Abdalla, A.N., Abdalla, M.A., Abdallah, E.M., Abdeeq, B.A., Abdel Razeq, N.M.I., Murray, C.J.L., 2025. Global burden of 292 causes of death in 204 countries and territories and 660 subnational locations, 1990–2023: a systematic analysis for the Global Burden of Disease Study 2023. Lancet 406 (10513), 1811–1872. https://doi.org/10.1016/S0140-6736(25)01917-8.

Nakornchai, S., Hopattaraput, P., Vichayanrat, T., 2016. Prevalence, severity and factors associated with dental fluorosis among children aged 8-10 years in Bangkok, Thailand. Southeast Asian J. Trop. Med Public Health 47 (5), 1105–1111. ⟨https://www.scopus.com/inward/record.uri?eid=2-s2.0-85024492893&partnerID=40&md5=2c83526d3f9258bedbef30c1e303ec58⟩.

Neurath, M.F., Artis, D., Becker, C., 2025. The intestinal barrier: a pivotal role in health, inflammation, and cancer. Lancet Gastroenterol. Hepatol. 10 (6), 573–592. https://doi.org/10.1016/s2468-1253(24)00390-x.

Nitayavardhana, I., Theerapanon, T., Srichomthong, C., Piwluang, S., Wichadakul, D., Porntaveetus, T., Shotelersuk, V., 2020. Four novel mutations of FAM20A in amelogenesis imperfecta type IG and review of literature for its genotype and phenotype spectra. Mol. Genet Genom. 295 (4), 923–931. https://doi.org/10.1007/s00438-020-01668-8.

Nowwarote, N., Osathanon, T., Kanjana, K., Theerapanon, T., Porntaveetus, T., Shotelersuk, V., 2019. Decreased osteogenic activity and mineralization of alveolar bone cells from a patient with amelogenesis imperfecta and FAM83H 1261G>T mutation. Genes Dis. 6 (4), 391–397. https://doi.org/10.1016/j.gendis.2019.07.005.

Nurbaeva, M.K., Eckstein, M., Feske, S., Lacruz, R.S., 2017. Ca^{2+} transport and signalling in enamel cells. J. Physiol. 595 (10), 3015–3039. https://doi.org/10.1113/jp272775.

Orchard, S., Ammari, M., Aranda, B., Breuza, L., Briganti, L., Broackes-Carter, F., Campbell, N.H., Chavali, G., Chen, C., del-Toro, N., Duesbury, M., Dumousseau, M., Galeota, E., Hinz, U., Iannuccelli, M., Jagannathan, S., Jimenez, R., Khadake, J., Lagreid, A., Hermjakob, H., 2013. The MIntAct project—IntAct as a common curation platform for 11 molecular interaction databases. Nucleic Acids Res. 42 (D1), D358–D363. https://doi.org/10.1093/nar/gkt1115.

Panneerselvam, K., Porras, P., del-Toro, N., Perfetto, L., Shrivastava, A., Ragueneau, E., Reyes, J.J.M., Orchard, S., Hermjakob, H., Curators, I.C., 2024. IntAct Database for Accessing IMEx's Contextual Metadata of Molecular Interactions. Curr. Protoc. 4 (10), e70018. https://doi.org/10.1002/cpz1.70018.

Pawłowska, N., Durda-Masny, M., Cofta, S., Springer, D., Szwed, A., 2025. Gut Dysbiosis Driven by CFTR Gene Mutations in Cystic Fibrosis Patients: From Genetic Disruption to Multisystem Consequences and Microbiota Modulation. Genes 16 (9), 1049. https://doi.org/10.3390/genes16091049.

Pei, F., Guo, T., Zhang, M., Ma, L., Jing, J., Feng, J., Ho, T.V., Wen, Q., Chai, Y., 2024. FGF signaling modulates mechanotransduction/WNT signaling in progenitors during tooth root development. Bone Res. 12 (1), 37. https://doi.org/10.1038/s41413-024-00345-5.

Pongsapipatana, N., Gavila, P., Cho, S.D., El-Tanani, M., Rabbani, S.A., Islam, S., Essigmann, J.M., Sriwattanapong, K., Porntaveetus, T., 2026. Urinary proteomic biomarkers of systemic fluoride exposure in children. Ecotoxicol. Environ. Saf. 309, 119643. https://doi.org/10.1016/j.ecoenv.2025.119643.

Porntaveetus, T., Oommen, S., Sharpe, P.T., Ohazama, A., 2010. Expression of Fgf signalling pathway related genes during palatal rugae development in the mouse. Gene Expr. Patterns 10 (4-5), 193–198. https://doi.org/10.1016/j.gep.2010.03.004.

Porntaveetus, T., Srichomthong, C., Ohazama, A., Suphapeetiporn, K., Shotelersuk, V., 2017. A novel GJA1 mutation in oculodentodigital dysplasia with extensive loss of enamel. Oral. Dis. 23 (6), 795–800. https://doi.org/10.1111/odi.12663.

Prawatvatchara, W., Intarak, N., Thaweesapphithak, S., Piamcharoen, T., Suwanchaikasem, P., Srinivasan, M., Porntaveetus, T., 2025. Comparative LC-MS analysis of monomer composition and elution from provisional and permanent 3D-printed dental resins. J. Dent. 165, 106262. https://doi.org/10.1016/j.jdent.2025.106262.

Pumchan, A., Gavila, P., Khieota, T., Jung, H.-S., Sriwattanapong, K., Porntaveetus, T., 2026. Salivary proteomic signatures reveal novel mechanistic insights into moderate dental fluorosis pathogenesis and oral homeostasis disruption. Comput. Struct. Biotechnol. J. 35 (1), 0003. https://doi.org/10.34133/csbj.0003.

Qiu, Y., Chen, X., Yan, X., Wang, J., Yu, G., Ma, W., Xiao, B., Quinones, S., Tian, X., Ren, X., 2020. Gut microbiota perturbations and neurodevelopmental impacts in offspring rats concurrently exposure to inorganic arsenic and fluoride. Environ. Int 140, 105763. https://doi.org/10.1016/j.envint.2020.105763.

Rawat, N., Sivanesan, S., Kanade, G.S., Bafana, A., 2025. Interaction of environmental fluoride exposure and gut microbes: potential implication in the development of fluorosis in human subjects. Food Chem. Toxicol. 200, 115388. https://doi.org/10.1016/j.fct.2025.115388.

Rodríguez-Piñeiro, A.M., Bergström, J.H., Ermund, A., Gustafsson, J.K., Schütte, A., Johansson, M.E., Hansson, G.C., 2013. Studies of mucus in mouse stomach, small intestine, and colon. II. Gastrointestinal mucus proteome reveals Muc2 and Muc5ac accompanied by a set of core proteins. Am. J. Physiol. Gastrointest. Liver Physiol. 305 (5), G348–G356. https://doi.org/10.1152/ajpgi.00047.2013.

Rojanaworarit, C., Claudio, L., Howteerakul, N., Siramahamongkol, A., Ngernthong, P., Kongtip, P., Woskie, S., 2021. Hydrogeogenic fluoride in groundwater and dental fluorosis in Thai agrarian communities: a prevalence survey and case–control study. BMC Oral. Health 21 (1), 545. https://doi.org/10.1186/s12903-021-01902-8.

Rosas López Portillo, F., Rosas Alcaraz, V.M., Gámez Valenzuela, J., Molina Ángulo, I.F., Gonzáles Jiménez, M.V., Olivas Velázquez, A.K., Reyna Solis, C.L., Rocha López, A., Cortina Aguilar, J.A., Villalobos Rodelo, J.J., Duque-Urióstegui, C., 2024. Dental fluorosis: a review. Int J. Res. Med. Sci. 12 (4), 1306–1310. https://doi.org/10.18203/2320-6012.ijrms20240663.

Rowland, M.A., Greenbaum, J.M., Deeds, E.J., 2017. Crosstalk and the evolvability of intracellular communication. Nat. Commun. 8 (1), 16009. https://doi.org/10.1038/ncomms16009.

Salati, S., Genovese, E., Carretta, C., Zini, R., Bartalucci, N., Prudente, Z., Pennucci, V., Ruberti, S., Rossi, C., Rontauroli, S., Enzo, E., Calabresi, L., Balliu, M., Mannarelli, C., Bianchi, E., Guglielmelli, P., Tagliafico, E., Vannucchi, A.M., Manfredini, R., 2019. Calreticulin Ins5 and Del52 mutations impair unfolded protein and oxidative stress responses in K562 cells expressing CALR mutants. Sci. Rep. 9 (1), 10558. https://doi.org/10.1038/s41598-019-46843-z.

Samaranayake, L., Porntaveetus, T., Tsoi, J., Tuygunov, N., 2025. Facts and fallacies of the fluoride controversy: a contemporary perspective. Int Dent. J. 75 (4), 100833. https://doi.org/10.1016/j.identj.2025.04.013.

Shannon, P., Markiel, A., Ozier, O., Baliga, N.S., Wang, J.T., Ramage, D., Amin, N., Schwikowski, B., Ideker, T., 2003. Cytoscape: a software environment for integrated models of biomolecular interaction networks. Genome Res. 13 (11), 2498–2504. https://doi.org/10.1101/gr.1239303.

Sharma, R., Tsuchiya, M., Bartlett, J.D., 2008. Fluoride induces endoplasmic reticulum stress and inhibits protein synthesis and secretion. Environ. Health Perspect. 116 (9), 1142–1146. https://doi.org/10.1289/ehp.11375.

Sherman, B.T., Hao, M., Qiu, J., Jiao, X., Baseler, M.W., Lane, H.C., Imamichi, T., Chang, W., 2022. DAVID: a web server for functional enrichment analysis and functional annotation of gene lists (2021 update). Nucleic Acids Res. 50 (W1), W216–w221. https://doi.org/10.1093/nar/gkac194.

Silva de Castilho, L., Ferreira e Ferreira, E., Perini, E., 2009. Perceptions of adolescents and young people regarding endemic dental fluorosis in a rural area of Brazil: psychosocial suffering. Health Soc. Care Community 17 (6), 557–563. https://doi.org/10.1111/j.1365-2524.2009.00859.x.

Skates, S.J., Gillette, M.A., LaBaer, J., Carr, S.A., Anderson, L., Liebler, D.C., Ransohoff, D., Rifai, N., Kondratovich, M., Težak, Ž., Mansfield, E., Oberg, A.L., Wright, I., Barnes, G., Gail, M., Mesri, M., Kinsinger, C.R., Rodriguez, H., Boja, E.S., 2013. Statistical design for biospecimen cohort size in proteomics-based biomarker discovery and verification studies. J. Proteome Res. 12 (12), 5383–5394. https://doi.org/10.1021/pr400132j.

Spencer, A.J., Do, L.G., Mueller, U., Baines, J., Foley, M., Peres, M.A., 2018. Understanding optimum fluoride intake from population-level evidence. Adv. Dent. Res 29 (2), 144–156. https://doi.org/10.1177/0022034517750592.

Sriwattanapong, K., Theerapanon, T., Khamwachirapitak, C., Sae-Ear, P., Sa-Ard-Iam, N., Shotelersuk, V., Porntaveetus, T., 2024. In-depth investigation of FAM20A insufficiency effects on deciduous dental pulp cells: altered behaviours, osteogenic differentiation, and inflammatory gene expression. Int. Endod. J. 57 (6), 745–758. https://doi.org/10.1111/iej.14056.

Sriwattanapong, K., Thaweesapphithak, S., Khamwachirapitak, C., Sae-Ear, P., Prommanee, S., Sa-Ard-Iam, N., Phothichailert, S., Jung, H.S., Shotelersuk, V., Porntaveetus, T., 2025. FAM20A deficiency drives transcriptomic dysregulation and functional impairment in gingival fibroblasts. Cell Prolif., e70096 https://doi.org/10.1111/cpr.70096.

Szklarczyk, D., Kirsch, R., Koutrouli, M., Nastou, K., Mehryary, F., Hachilif, R., Gable, A. L., Fang, T., Doncheva, N.T., Pyysalo, S., Bork, P., Jensen, L.J., von Mering, C., 2023. The STRING database in 2023: protein-protein association networks and functional enrichment analyses for any sequenced genome of interest. Nucleic Acids Res. 51 (D1), D638–d646. https://doi.org/10.1093/nar/gkac1000.

Techawiwattanaboon, T., Phanchamnan, E., Iadsee, N., Makjaroen, J., Pisitkun, T., Patarakul, K., 2023. Proteomic profile of naturally released extracellular vesicles secreted from Leptospira interrogans serovar Pomona in response to temperature and osmotic stresses. Sci. Rep. 13 (1), 18601. https://doi.org/10.1038/s41598-023-45863-0.

Ting, L., Cowley, M.J., Hoon, S.L., Guilhaus, M., Raftery, M.J., Cavicchioli, R., 2009. Normalization and statistical analysis of quantitative proteomics data generated by metabolic labeling. Mol. Cell Proteom. 8 (10), 2227–2242. https://doi.org/10.1074/mcp.M800462-MCP200.

Villaveces, J.M., Jiménez, R.C., Porras, P., del-Toro, N., Duesbury, M., Dumousseau, M., Orchard, S., Choi, H., Ping, P., Zong, N.C., Askenazi, M., Habermann, B.H., Hermjakob, H., 2015. Merging and scoring molecular interactions utilising existing community standards: tools, use-cases and a case study. Database 2015. https://doi.org/10.1093/database/bau131.

Visser, E.A., Moons, S.J., Timmermans, S., de Jong, H., Boltje, T.J., Büll, C., 2021. Sialic acid O-acetylation: From biosynthesis to roles in health and disease. J. Biol. Chem. 297 (2), 100906. https://doi.org/10.1016/j.jbc.2021.100906.

Wang, J., Yu, C., Zhang, J., Liu, R., Xiao, J., 2023. Aberrant gut microbiota and fecal metabolites in patients with coal-burning endemic fluorosis in Guizhou, China. Environ. Sci. Pollut. Res. 30 (27), 69913–69926. https://doi.org/10.1007/s11356-023-27051-9.

Wang, Y., Xu, J., Chen, H., Shu, Y., Peng, W., Lai, C., Kong, R., Lan, R., Huang, L., Xin, J., Sun, N., Ni, X., Bai, Y., Wu, B., 2023. Effects of prolonged fluoride exposure on innate immunity, intestinal mechanical, and immune barriers in mice. Res Vet. Sci. 164, 105019. https://doi.org/10.1016/j.rvsc.2023.105019.

Wei, W., Gao, Y., Wang, C., Zhao, L., Sun, D., 2013. Excessive fluoride induces endoplasmic reticulum stress and interferes enamel proteinases secretion. Environ. Toxicol. 28 (6), 332–341. https://doi.org/10.1002/tox.20724.

Williams, T.D., Michalak, E.M., Carey, K.T., Lam, E.Y.N., Anderson, A., Griesbach, E., Chan, Y.-C., Papasaikas, P., Tan, V.W.T., Ngo, L., MacPherson, L., Gilan, O., Rucinski, A., Rutkowska-Klute, A., Zinn, N., Grandi, P., Bantscheff, M., Prinjha, R.K., Dawson, S.-J., Dawson, M.A., 2025. mRNA export factors store nascent transcripts within nuclear speckles as an adaptive response to transient global inhibition of

transcription. Mol. Cell 85 (1), 117–131. https://doi.org/10.1016/j.molcel.2024.12.008.

Wongong, R., Kijtawornrat, A., Srichomthong, C., Tongkobpeth, S., Od-Ek, P., Assawapitaksakul, A., Caengprasath, N., Khongphatthanayothin, A., Porntaveetus, T., Shotelersuk, V., 2024. A novel BAG5 variant impairs the ER stress response pathway, causing dilated cardiomyopathy and arrhythmia. Sci. Rep. 14 (1), 11980. https://doi.org/10.1038/s41598-024-62764-y.

Xu, J., Su, X., Burley, S.K., Zheng, X.F.S., 2022. Nuclear SOD1 in Growth Control, Oxidative Stress Response, Amyotrophic Lateral Sclerosis, and Cancer. Antioxidants 11 (2), 427. https://doi.org/10.3390/antiox11020427.

Xu, K., Huang, R., Wen, R., Yao, T., Cao, Y., Chang, B., Cheng, Y., Yi, X., 2024. Annexin A family: A new perspective on the regulation of bone metabolism. Biomed. & Pharmacother. 178, 117271. https://doi.org/10.1016/j.biopha.2024.117271.

Yamaguchi, H., Meyer, M.D., He, L., Komatsu, Y., 2022. Disruption of Trip11 in cranial neural crest cells is associated with increased ER and Golgi stress contributing to skull defects in mice. Dev. Dyn. 251 (7), 1209–1222. https://doi.org/10.1002/dvdy.461.

Yasin, M., Zohoori, F.V., Kumah, E.A., Subramanian, M., Dean, P., Orr, C.H., 2025. Effect of fluoride on gut microbiota: a systematic review. Nutr. Rev. 83 (7), e1853–e1880. https://doi.org/10.1093/nutrit/nuae202.

Yoo, D.Y., Cho, S.B., Jung, H.Y., Kim, W., Lee, K.Y., Kim, J.W., Moon, S.M., Won, M.H., Choi, J.H., Yoon, Y.S., Kim, D.W., Choi, S.Y., Hwang, I.K., 2019. Protein disulfide-isomerase A3 significantly reduces ischemia-induced damage by reducing oxidative and endoplasmic reticulum stress. Neurochem. Int 122, 19–30. https://doi.org/10.1016/j.neuint.2018.11.002.

Zhang, Y., Li, W., Chi, H.S., Chen, J., Denbesten, P.K., 2007. JNK/c-Jun signaling pathway mediates the fluoride-induced down-regulation of MMP-20 in vitro. Matrix Biol. 26 (8), 633–641. https://doi.org/10.1016/j.matbio.2007.06.002.

Zhong, N., Ma, Y., Meng, X., Sowanou, A., Wu, L., Huang, W., Gao, Y., Pei, J., 2022. Effect of fluoride in drinking water on fecal microbial community in rats. Biol. Trace Elem. Res. 200 (1), 238–246. https://doi.org/10.1007/s12011-021-02617-1.

Zhou, G., Li, Q., Hou, X., Wu, H., Fu, X., Wang, G., Ma, J., Cheng, X., Yang, Y., Chen, R., Li, Z., Yu, F., Zhu, J., Ba, Y., 2023. Integrated 16S rDNA sequencing and metabolomics to explore the intestinal changes in children and rats with dental fluorosis. Ecotoxicol. Environ. Saf. 251, 114518. https://doi.org/10.1016/j.ecoenv.2023.114518.

Zhu, S., Liu, J., Han, B., Zhao, W., Zhou, B., Zhao, J., Wang, H., 2022. Fluoride exposure cause colon microbiota dysbiosis by destroyed microenvironment and disturbed antimicrobial peptides expression in colon. Environ. Pollut. 292, 118381. https://doi.org/10.1016/j.envpol.2021.118381.